Watershed sediment supply and potential impacts of dam removals for an estuary

David Ralston[1], Brian Yellen[2], and Jonathon Woodruff[2]

[1]Woods Hole Oceanographic Institution
[2]University of Massachusetts, Amherst

November 26, 2022

Abstract

Observations and modeling are used to assess potential impacts of sediment releases due to dam removals on the Hudson River estuary. Watershed sediment loads are calculated based on sediment-discharge regressions for gauges covering 80% of the watershed area. The annual average sediment load to the estuary is 1.2 Mt, of which about 0.6 Mt comes from tributaries entering below the head of tides. Sediment yield varies inversely with watershed area, with regional trends that are consistent with differences in substrate erodibility. Geophysical and sedimentological surveys in five subwatersheds of the Lower Hudson were conducted to characterize the mass and composition of sediment trapped behind dams. Impoundments were classified as 1) active sediment traps, 2) run-of-river sites not actively trapping, and 3) dammed natural lakes and spring-fed ponds. Based on this categorization and impoundment attributes from the dam inventory database, the total mass of impounded sediment in the Lower Hudson watershed is estimated as 3.1 Mt. Assuming that roughly half of the impounded sediment is typically released downstream with dam removal, then the potential inputs represent less than 2 years of annual watershed supply. Modeling of simulated dam removals shows that modest suspended sediment increases occur in the estuary within about a tidal excursion of the source tributary, primarily during discharge events. Transport in the estuary depends strongly on settling velocity, but fine particles, which are important for accretion in tidal wetlands, deposit broadly along the estuary rather than primarily near the source.

1

1 **Watershed sediment supply and potential impacts of dam removals for an estuary**

2 David K. Ralston[1*], Brian Yellen[2], Jonathon D. Woodruff[2]

3

4 [1] Woods Hole Oceanographic Institution, Woods Hole, MA, USA

5 [2] University of Massachusetts, Amherst, MA, USA

6

7 Submitted to *Estuaries and Coasts*

8 March 13, 2020

9 *corresponding author: dralston@whoi.edu, 508-289-2587

10 **ABSTRACT**

11 Observations and modeling are used to assess potential impacts of sediment releases due to dam removals
12 on the Hudson River estuary. Watershed sediment loads are calculated based on sediment-discharge
13 regressions for gauges covering 80% of the watershed area. The annual average sediment load to the
14 estuary is 1.2 Mt, of which about 0.6 Mt comes from tributaries entering below the head of tides.
15 Sediment yield varies inversely with watershed area, with regional trends that are consistent with
16 differences in substrate erodibility. Geophysical and sedimentological surveys in five subwatersheds of
17 the Lower Hudson were conducted to characterize the mass and composition of sediment trapped behind
18 dams. Impoundments were classified as 1) active sediment traps, 2) run-of-river sites not actively
19 trapping, and 3) dammed natural lakes and spring-fed ponds. Based on this categorization and
20 impoundment attributes from the dam inventory database, the total mass of impounded sediment in the
21 Lower Hudson watershed is estimated as 3.1 Mt. Assuming that roughly half of the impounded sediment
22 is typically released downstream with dam removal, then the potential inputs represent less than 2 years
23 of annual watershed supply. Modeling of simulated dam removals shows that modest suspended sediment
24 increases occur in the estuary within about a tidal excursion of the source tributary, primarily during
25 discharge events. Transport in the estuary depends strongly on settling velocity, but fine particles, which
26 are important for accretion in tidal wetlands, deposit broadly along the estuary rather than primarily near
27 the source.

28 **Keywords:** dam removal, suspended sediment, watershed sediment yield, sediment supply, sediment
29 trapping

30 **1. Motivation and background**

31 Dam removal is occurring at an accelerating pace around the United States, motivated by various goals
32 including improving aquatic connectivity, mitigating safety risks, or removing structures that no longer
33 serve their intended purpose (O'Connor et al. 2015). In many cases, an important consideration in dam
34 removal is the potential environmental impacts associated with release of sediment that has accumulated
35 in the impoundment while the dam was in place (Grant and Lewis 2015; Foley et al. 2017). Impounded
36 sediment can be excavated and taken away prior to dam removal and potentially put to beneficial use, but
37 this approach is often prohibitively expensive, so instead sediment is allowed to erode and be transported
38 downstream by flow in the tributary (Pizzuto 2002). Most dam removals are small (e.g., dam height < 10
39 m, impounded sediment volume < 10,000 m^3), so the environmental impacts downstream are relatively
40 modest (Sawaske and Freyberg 2012; Tullos et al. 2016). However, removal of large dams has become
41 increasingly common and the associated downstream impacts can extend over greater distance and time
42 (Warrick et al. 2015; Foley et al. 2017). Effects of dam removals large or small are typically studied in
43 isolation. The increasing interest in dam removals raises questions about potential cumulative impacts at
44 the watershed scale.

45 After dam removal, suspended sediment concentrations in the waterway downstream can increase by a
46 factor of 10 or more, but in most cases sediment concentrations are only elevated for a few weeks to
47 months (Doyle et al. 2003; Ahearn and Dahlgren 2005; Riggsbee et al. 2007; Major et al. 2012; Wilcox et
48 al. 2014). The relative increase in turbidity, or reduction in water clarity associated with suspended
49 sediment, is sensitive to the fraction of fine sediment in the impoundment, as coarser sediments like sand
50 and gravel are less likely to be transported in suspension (Wilcox et al. 2014). The increase in turbidity
51 following dam removal is often similar to that during large discharge events (Tullos et al. 2016), but the
52 turbidity increase can be greater compared to background if the removal occurs during a period of low to
53 moderate discharge (Magirl et al. 2015). Finer sediment (clay, silt, fine sand) typically moves farther

54 downstream than coarse sand and gravel, and the coarser fraction typically deposits within a few km
55 downstream of the dam (Major et al. 2012; Wilcox et al. 2014; Magirl et al. 2015; Magilligan et al. 2016).
56 The distance downstream of coarse sediment aggradation has been found to depend on the ratio of the
57 impounded sediment volume to the annual watershed sediment input, but this ratio has not been observed
58 to correlate with deposition of finer sediment (Grant and Lewis 2015).

59 A majority of the sediment eroded from an impoundment occurs in the first few months after dam
60 removal (Doyle et al. 2003; Pearson et al. 2011; Sawaske and Freyberg 2012; Collins et al. 2017).
61 Notably, the total volume of sediment eroded does not depend strongly on the discharge conditions after
62 dam removal, but instead depends primarily on the removal method and sediment characteristics, in
63 particular grain size and cohesiveness (Grant and Lewis 2015; Magilligan et al. 2016; Collins et al. 2017;
64 Foley et al. 2017). Less sediment is eroded for gravel-filled impoundments (30-40%) than for sand (40-
65 70%), and phased dam removals have less sediment eroded (10-40%) than rapid breaching (30-70%)
66 (Grant and Lewis 2015; Tullos et al. 2016; Foley et al. 2017). Cohesive sediment is generally more
67 resistant to erosion than sand due to consolidation after dewatering, but a dam removal with a rapid
68 breach and no dewatering resulted in mobilization of about 60% of the impounded fine sediment (Wilcox
69 et al. 2014).

70 Much of the research on dam removal has focused on fluvial geomorphology and ecology impacts (Tullos
71 et al. 2016; Foley et al. 2017). Few studies have examined potential impacts on coastal or estuarine waters
72 farther downstream, although studies of two major dam removals on tributaries of the tidal Columbia
73 River note that a significant fraction of the fine sediment passed through the fluvial channels and went
74 into the estuary (Major et al. 2012; Wilcox et al. 2014). One of the largest dam removals to date was on
75 the Elwha River (WA), and it included monitoring of conditions where it discharges into the coastal
76 ocean (Warrick et al. 2015). The Elwha involved phased removals of two dams, and about 35% of the
77 impounded sediment had been eroded 2 years after the removal process began. Of the sediment removed,
78 about 90% passed through the fluvial section to the coastal ocean, and about half of that was deposited in
79 the delta at the mouth (Warrick et al. 2015). The dam removal resulted in a deposition rate in the
80 submarine delta that was about 100 times greater than before removal (Gelfenbaum et al. 2015).
81 Deposition was strongly grain-size dependent, with about 70% of the sand and gravel that made it to the
82 coast depositing within 2 km of the mouth compared to 6% of the mud due to strong tidal currents at the
83 mouth (Gelfenbaum et al. 2015). In the fluvial channel, the sediment transport was 3 and 20 times the
84 average annual load in years 1 and 2 respectively, and during high discharge events the suspended
85 sediment concentrations increased to several thousand mg/L (Magirl et al. 2015).

86 Increases in sediment concentrations and deposition rates after dam removal can have adverse ecosystem
87 impacts. For example, the high deposition rates near the mouth of the Elwha were linked to reductions in
88 macroalgae and changes in the abundance of invertebrate and fish taxa (Rubin et al. 2017). This reduction
89 in macroalgae was associated with decreases in light availability (Glover et al. 2019). Submerged
90 vegetation can also be negatively impacted by increased turbidity following sediment inputs from extreme
91 discharge events, as with Tropical Storm Agnes in Chesapeake Bay (Orth and Moore 1984) and Tropical
92 Storms Irene and Lee in the Hudson River estuary (Hamberg et al. 2017).

93 However, increases in coastal sediment inputs are not necessarily harmful, and in many cases can have
94 beneficial impacts. In regions with limited sediment supply, additional sediment inputs due to dam
95 removals or storm events can help mitigate shoreline erosion and promote marsh resilience (Ganju et al.
96 2013; Ganju 2019). For the Elwha, the shoreline near the river mouth was erosional prior to dam removal,
97 but the subsequent increase in sediment supply has, over a period of about 5 years, reversed this trend and
98 led to accretion on upcoast and downcoast beaches (Warrick et al. 2019). The timescales for adjustment to

99   changes in sediment input can be long depending on sediment availability. For example, sediment loading
100 to San Francisco Bay increased substantially with hydraulic mining in the late 1800s and then decreased
101 with the building of major dams in the middle of the 20th century, but the response of turbidity in the
102 estuary lagged these input shifts as the mobile pool of sediment available for resuspension adjusted over
103 time scales of decades (Schoellhamer 2011). Similarly, the ecosystem response lagged changes in
104 sediment supply by decades, including changes in phytoplankton, fish, and submerged vegetation with
105 water clarity (Schoellhamer et al. 2013).

106 Potential impacts of dam removals on coastal and estuarine regions, whether positive or negative, are of
107 increasing interest scientifically and for environmental management. Dam removal regulators and
108 practitioners need to assess potential impacts of sediment releases and develop mitigation strategies.
109 Environmental managers want to minimize potential harmful effects but also assess whether increased
110 sediment loading may aid in resilience of coastal wetlands to sea level rise. Most dam removals are
111 relatively small and thus unlikely to support extensive study and monitoring, but the cumulative effect of
112 many small dam removals may be significant when compared to the background sediment loading from
113 the watershed, which itself is rarely well known.

114 This study presents an integrated approach for assessing impacts of dam removals on an estuary, with the
115 Hudson River estuary as a study site. The research questions are multidisciplinary and thus so are the
116 methodologies, but this integrated approach is necessary to develop the context for assessing potential
117 positive or negative impacts. Sediment inputs from dam removals can increase turbidity and accretion in
118 the estuary, and we assess the spatial and temporal extent of this increase. We assess how transport in the
119 estuary depends on sediment grain size, and relate this to the sediment grain sizes found in neighboring
120 tidal wetlands and representative upstream impoundments. The approach mixes observations and
121 modeling, and the results should be transferable to other estuaries with similar forcing and sediment
122 characteristics.

2. Site description

124 Tides extend 240 km up the Hudson River from The Battery in New York City until just below the
125 confluence of the Mohawk and Upper Hudson Rivers in Troy, NY. The limit of salinity intrusion in the
126 estuary varies seasonally with river discharge, from around Piermont (40 km from The Battery, or 40
127 rkm) during high flow to near Poughkeepsie (120 rkm) during extreme low discharge (Bowen and Geyer
128 2003; Ralston et al. 2008). The Mohawk and Upper Hudson combine for a mean discharge of about 420
129 $m^3 s^{-1}$. Smaller tributaries flowing directly into the tidal Hudson increase this by 30-60% (Lerczak et al.
130 2006; Wall et al. 2008). Discharge from the Upper Hudson and Mohawk during the spring freshet is
131 typically around 2000 $m^3 s^{-1}$, and summer low discharge can be less than 100 $m^3 s^{-1}$. Mean tidal range is
132 about 1.4 m at The Battery, decreasing to 1 m around West Point (90 rkm) and increasing to 1.6 m at the
133 tidal limit at Troy, NY (Ralston et al. 2019).

134 Bed sediment in the upper 60 km of the tidal river is predominately sand and it is muddier in the middle
135 and lower estuary, but the bed composition is heterogeneous throughout the estuary (Nitsche et al. 2007).
136 Suspended sediment concentrations (SSC) in the estuary increase during high river discharge and spring
137 tides. In the tidal river, SSC can be several hundred mg/L during discharge events and decrease by a
138 factor of 10 during lower discharge periods. Through spring-neap cycles, SSC can vary by a factor of 2 or
139 more (Wall et al. 2008; Ralston and Geyer 2017). In the saline estuary, bottom salinity fronts result in
140 multiple estuarine turbidity maxima (ETM) with several hundred to 1000 mg/L, most prominently near
141 the constriction at the George Washington Bridge (around 20 rkm) and upstream from Croton Point in
142 Haverstraw Bay (around 60 rkm) (Geyer et al. 2001; Ralston et al. 2012).

This study focuses on three regions of the estuary near tidal marshes that are part of the Hudson River National Estuarine Research Reserve (HRNERR) and their associated side tributaries (Fig. 1): 1) Claverack and Kinderhook watersheds that discharge into the tidal Hudson near Stockport Flats marsh (193 rkm); 2) Esopus, Saw Kill, and Stony Creek watersheds that discharge near Tivoli Bays marshes (158 rkm); and 3) Doodletown Brook, Peekskill Hollow Creek, and Popolopen Creek watersheds that discharge near Iona Island marsh (72 rkm). The study sites were selected to represent a range of watershed and estuary conditions. The upper two sites are located in the tidal fresh river, whereas the river at Iona Island is fresh during moderate to high river discharge and brackish at low discharge.

Geology differs considerably across the Lower Hudson watershed. In the southern part, the bedrock is dominated by crystalline, high-grade metamorphic rock (Dicken et al. 2005), with generally thin sandy soils (Olsson 1981). Soils in Claverack Creek watershed are dominated by extensive lacustrine silts and clays, with highly variable underlying material derived from slices of marine sedimentary rocks and low-grade metamorphic rocks from the Taconic Orogeny (Faber 2002). West of the Hudson, clastic sedimentary rocks make up most of the Catskill Mountains (Dicken et al., 2005), with spatially limited exposures of glaciolacustrine clays contributing significant sediment to upland streams (McHale and Siemion 2014).

3. Methods

3.1 Geophysical measurements

Starting with the US Army Corps National Inventory of Dams (NID) database, we selected impoundment study sites from five watersheds that have prominent tidal marshes at their mouths. Based on remote observation and data from the NID database, we categorized dams with respect to their ability to trap sediment into three groups. Group 1 dam impoundments trap greater than an estimated 10% of incoming sediment, as calculated by the widely used Brune method (Brune 1953), and are classified as effective sediment traps. Group 2 dam impoundments had a ratio of impoundment width to river width of less than 2 and classified as run-of-river with limited sediment storage capacity (many confirmed with satellite photos showing impoundments full of sediment). Group 3 includes three types of dams that have minimal effect on watershed sediment processes, including natural lakes with a dammed outlet, breached dams, and upland spring-fed ponds with small watersheds (< 2 km^2) void of a significant inlet stream.

A total of 17 impoundments across five tributary watersheds were surveyed in the field for sediment mass, accumulation rate, and grain size. Impoundments were chosen to represent a range of upstream watershed sizes, land cover, and underlying geology. We preferentially selected dams that trap most of the incoming sediment load based on the ratio of watershed size to impoundment volume, but also evaluated three dams that trap little sediment due to minimal accommodation space and short residence time at high flows. At each site, a minimum of three sediment cores were collected in a transect from inlet to dam. Water depths were surveyed via canoe with an acoustic bathymetric profiler. Depths were interpolated between measurements using the open source Quantum GIS (QGIS) triangular irregular network tool and the average depth of the interpolated data was multiplied by impoundment surface area to estimate water volume. Sediment cores were sampled every 10 cm and above and below notable lithologic transitions. The change in mass during drying was recorded to estimate porosity, assuming initially saturated samples. Samples were then combusted at 550 °C for 4 hours to estimate organic fraction (Dean 1974), with the remaining mass constituting the clastic portion. After removing organics by combustion, samples were gently disaggregated by mortar and pestle and run on a Coulter laser diffraction particle size analyzer. Clastic mass was divided by initial sample volume, which was estimated using a density of 1.2 and 2.65 g/cc for organic and clastic material respectively (Avnimelech et al. 2001).

187   Dry bulk density values from the centrally located sediment core in each impoundment were averaged to
188   estimate a representative value of clastic mass per cubic meter of sediment. Average sediment thickness
189   for each site was based on core stratigraphy and supported by extensive probing. The site-averaged
190   sediment thickness was multiplied by impoundment area and site averaged dry bulk density to compute
191   total clastic mass in each impoundment. Historical records and the NID database were used to date
192   impoundment construction to calculate a rate of sediment mass accumulation. When historical records
193   were not available, we use the 1954 CE ^{137}Cs onset to constrain sediment accumulation rates (Pennington
194   et al. 1973). Within the tidal wetland at the mouth of each of the five tributaries, we collected a transect of
195   cores to constrain the developmental history and accumulation rates at each site using similar methods as
196   described above (Yellen et al., submitted).

197   Based on the sediment trapping characteristics of each of the three dam classes, we applied rules to scale
198   up these observations to include every dam within each study watershed. Sediment stored within
199   impoundments classified as "active traps" was quantified by applying a regional sediment yield to the
200   upstream watershed area and age of the dam and then adjusted downward based on the Brune (1953)
201   trapping efficiency of the dam. For run of river dams, we approximated average sediment depth as 35%
202   the MID-listed dam height. This sediment thickness was multiplied by the impoundment area and an
203   average value of clastic mass per unit volume from directly observed sites to convert to sediment mass.
204   We assumed zero trapped sediment within our Group 3 (non-source) dams as a removal of a dam of this
205   type would not result in any sediment being transported downstream.

206   *3.2 Discharge and sediment monitoring*

207   We used daily sediment discharge observations from USGS river gauging stations to characterize
208   sediment loading to the Hudson River estuary (Fig. 1, Table 1). The two largest tributaries, the Mohawk
209   (Cohoes, 01357500) and Upper Hudson (Waterford, 01335770), enter just upstream from the tidal limit.
210   Gauges near the mouths of smaller tributaries that flow directly into the lower Hudson include Catskill
211   (01362090), Kinderhook (01361000), Roeliff Jansen (01362182), and Rondout (01362182). The Esopus
212   watershed includes the Ashokan Reservoir, which is the second largest reservoir in the New York City
213   drinking water supply system (Mukundan et al. 2013). Gauges upstream of the reservoir include the
214   Esopus tributary Stony Clove (01362370) and the Esopus at Coldbrook (01362500), and downstream
215   gauges were on the Esopus at Lomontville (01363556) and Mount Marion (01364500). The Rondout
216   River also contains a large drinking water supply reservoir, which impounds 8% of its watershed. In
217   addition to its 246 km^2 watershed, the Rondout Reservoir receives water from the Delaware Basin and
218   exports water for ultimate distribution to New York City. Data from Schoharie Creek (01351500), a
219   tributary of the Mohawk that enters just upstream of Cohoes, are also included because it represents a
220   significant sediment source and is representative of other subwatersheds in the Catskills that discharge
221   directly to the tidal Hudson. Record lengths for discharge varied from more than 100 years to 4 years.
222   Sediment discharge record lengths for most sites were brief (<5 years), except for the Upper Hudson and
223   Mohawk that have several decades of sediment data (Fig 2).

224   To relate sediment load (Q_s) to volumetric freshwater discharge (Q_r) we use a locally weighted scatter
225   smoothing, or LOWESS approach (Cleveland 1979; Helsel and Hirsch 2002). An alternative to a
226   regression of $Q_s = a\ Q_r^b$ (Nash 1994), the LOWESS approach is well suited to data which have curvature
227   in the relationship between discharge and sediment load (Hicks et al. 2000; Warrick et al. 2013).
228   LOWESS fits between $\log_{10}(Q_r)$ and $\log_{10}(Q_s)$ were calculated for each gauging station using a smoothing
229   factor of $f = 0.2$ (Fig. 3). Similar results were found for $f = 0.1$ and 0.3. Sediment loads were calculated
230   from the fits and input Q_r, including a bias correction factor to account for the conversion from log-
231   transformed variables (Ferguson 1986; Cohn 1995). The bias correction has the form $Q_s = 10^{\wedge}(C_{out} +$

232 $\sigma^2/2$), where C_{out} is the output from the LOWESS regression to $\log_{10}(Q_r)$ and σ^2 is the variance in the
233 residual of the fit. The correction resulted in an increase on the uncorrected sediment load for most
234 stations by a factor between 1.1 to 1.3. Linear regressions were also calculated between $\log_{10}(Q_r)$ and
235 $\log_{10}(Q_s)$, fitting high and low discharge regimes separately (Nash 1994; Woodruff 1999). Overall
236 however, the LOWESS fits had higher correlation and skill score ($r^2 = 0.98$, SS=0.98, Fig. 3) than the
237 bilinear regression approach ($r^2 = 0.89$, SS=0.89).

3.3 Sediment transport model

239 A hydrodynamic and sediment transport model was used to assess the fate of sediment in the estuary from
240 simulated dam removals. The model uses the Coupled Ocean–Atmosphere–Wave–Sediment Transport
241 (COAWST) modeling system (Warner et al. 2010), and configuration for the Hudson has been developed
242 and evaluated against observations in previous studies (Ralston et al. 2012; Ralston et al. 2013; Ralston
243 and Geyer 2017). The domain has open boundaries in New York Bight and Western Long Island Sound
244 and includes all the tidal Hudson. River inputs are prescribed at the head of tides and at seven smaller
245 tributaries based on USGS data as described above.

246 To simulate the effects of an increase in sediment supply from dam removal, several model scenarios
247 were run using realistic discharge and tidal forcing. Sediment inputs to the model are based on the
248 regressions between mean SSC (equivalent to Q_s/Q_r) and Q_r for the tributaries. We represent expected
249 sediment loading from potential dam removals by multiplying Q_s vs. Q_r regression results by a factor of 3
250 based on field observations of monitored dam removals (Doyle et al. 2003; Ahearn and Dahlgren 2005;
251 Riggsbee et al. 2007; Magirl et al. 2015). While SSC in the tributary downstream can increase by a factor
252 of 10 or more immediately after dam breaching (Doyle et al. 2003; Wilcox et al. 2014), concentrations
253 decrease after an initial adjustment period. For example, sediment concentrations during discharge events
254 several months after a dam removal were 1.2-1.8 times greater than before, and only within 10 km
255 downstream (Riggsbee et al. 2007). Many factors contribute to sediment availability in the impoundment
256 and downstream transport, including the dam removal process, slope, sediment grain size, and
257 impoundment geometry (Riggsbee et al. 2007; Grant and Lewis 2015; Foley et al. 2017), and we do not
258 address the range of potential scenarios here, nor do we account for fluvial transport processes between
259 the impoundment and the estuary. The factor of 3 increase is taken to be a representative value, with the
260 understanding that estuarine impacts will approximately scale with this sediment input for specific cases.

261 To evaluate potential impacts for a range of river discharge conditions, several periods were simulated
262 with realistic forcing. The simulation periods were selected because they had previously been evaluated
263 against observations of water level, velocity, salinity, and suspended sediment in the estuary. Results
264 presented here focus on the spring and summer of 2014, which had a typical spring freshet followed by
265 lower discharge summer (Ralston and Geyer 2017). Additional simulations included a winter with lower
266 than average discharge in 2015 and high discharge events in 2011, but these gave qualitatively similar
267 results with respect to the dispersal of dam removal sediment and so are not presented here. Scenarios
268 were also run to represent sediment releases from various locations along the estuary, with sediment
269 releases from tributaries corresponding to the impoundment and marsh observations described above
270 including: Kinderhook Creek near Stockport Marsh (193 rkm), Esopus Creek near Tivoli Marsh (160
271 rkm), and Doodletown Brook near Iona Island Marsh (70 rkm) (Fig. 1). Discharge and sediment
272 measurements from USGS gauges were used to force the Kinderhook and Esopus sediment release
273 locations, and for Doodletown Brook synthetic time series were used based on gauged watersheds of
274 similar size.

4. Results

4.1 Watershed sediment yield

An understanding of the sediment inputs from the watershed is essential for context to assess potential impacts of sediment from dam removals on the estuary downstream. Watershed sediment yield, or mass of sediment per watershed area per time, is highly variable between catchments and with time, depending on factors such as watershed slope, underlying geology, and land use (Syvitski et al. 2000). For example, steeper watersheds produce more sediment per unit area than low gradient regions, and intensive agriculture increases yields compared with forested land (Smith and Wilcock 2015). Sediment yields also depend inversely on watershed area (Milliman and Syvitski 1992). Larger watersheds have more areas for long-term sediment storage such as low-gradient floodplains and thus export less sediment per unit area. Here we use monitoring data to assess the sediment load to the Hudson estuary and provide context for potential loading from dam removals.

Most of the sediment observations in gauged tributaries are relatively recent (since 2011) and brief (< 5 years) (Fig. 2). The longest records are from the Mohawk at Cohoes, which has data from 1954-1959, 1976-1979, and 2004-2018, and the Upper Hudson at Waterford, with data from 1976-2014. The Hudson watershed has been significantly altered by humans for centuries, but most of the major changes in land use occurred prior to the start of sediment monitoring (Swaney et al. 2006). For some of the gauging stations, the volumetric discharge measurements span a period longer than the sediment monitoring. To incorporate the longer discharge records, sediment yields are calculated based on the Q_s vs. Q_r regressions (Fig. 3) using Q_r both during the sediment load measurements and for the full Q_r record.

The observed and calculated sediment yields vary inversely with watershed area (Fig. 4). Sediment yields for the largest watersheds, the Upper Hudson and Mohawk, average 16 and 51 t km^{-2} yr^{-1} respectively based on observed values and adjust down slightly when using long-term Q_r regressions to 13 and 41 t km^{-2} yr^{-1} (Table 1). Previously reported sediment yields ranged from 8 to 27 t km^{-2} yr^{-1} for Upper Hudson and 30 to 70 t km^{-2} yr^{-1} for the Mohawk (Wall et al. 2008). The Mohawk watershed is smaller and to the west of the Upper Hudson, with fine grained clastic sedimentary bedrock and extensive agriculture in its broad valley. The Upper Hudson, in contrast, is more forested and underlain by crystalline metamorphic rock (Phillips and Hanchar 1996). Lower Hudson tributary watersheds draining from the west, largely within the Catskill Mountains, and generally have higher sediment yields than those draining from the east (Fig. 4). For example, Catskill Creek, which drains the Catskill Mountains to the west of the Hudson, and Kinderhook Creek, which drains the Taconic Mountains to the east, have similar watershed areas (850 and 1050 km^2), percent forest cover (75% and 81%) and average basin slopes, but the observed and calculated sediment yields for Catskill Creek are 3 to 6 times greater (Fig. 4, Table 1).

The smallest watershed with suspended sediment measurements was Stony Clove, a tributary of Esopus Creek, and it had the highest observed yield. For Stony Clove, the yield based on the full discharge record (1930 t km^2 yr^{-1}, 1997-2019) was much greater than observed directly (68 t km^{-2} yr^{-1}, 2011-2014). The sediment observations occurred during a period with few large discharge events (none greater than 30 m^3 s^{-1}), in stark contrast to the discharge observations preceding that (27 events exceeding 30 m^3 s^{-1} in the 10 years prior, Fig. 2h). Similar variability in the frequency and magnitude of discharge events over this period was seen at other sites (e.g., Schoharie, Esopus at Coldbrook, Esopus at Mount Marion), and the large difference in calculated yields for Stony Clove reflects the extreme sensitivity of sediment discharge to Q_r and the sharp differences in discharge conditions. Downstream at Coldbrook on the Esopus, the watershed area is greater than Stony Clove by a factor of 6 and the observed yield is lower, consistent with the overall trend with watershed area (97 t km^{-2} yr^{-1} observed, 199 t km^{-2} yr^{-1} based on all discharge). Even farther downstream on the Esopus at Lomontville and Mount Marion, the watershed areas are about 1.5 and 2 times larger than at Coldbrook, and the sediment yields decrease by a factor of 10 to 20 (4 and

321 13 t km^{-2} yr^{-1} observed, 5 and 54 t km^{-2} yr^{-1} from all discharge). The sharp decrease in sediment yield at
322 the lower two stations is due in part to trapping by the Ashokan Reservoir, and as a result those fall well
323 below the yield-vs-area trend for other locations.

324 The relationship between sediment yield (Y) and watershed area (A) can be represented as a power law,

325 $$Y = cA^d \qquad (1)$$

326 where c and d are coefficients found by linear regression of $\log_{10}(Y)$ and $\log_{10}(A)$ (Milliman and Syvitski
327 1992). The sediment yields using the full Q_r records were fit all together, as well as separately for the
328 watersheds east and west of the Hudson to account for the differences in lithology (Fig. 4, Table 2). The
329 resulting fit coefficients are comparable to those from a global assessment, which found for "upland"
330 rivers (maximum elevation 500-1000 m) $c = 12$ and $d = -0.59$ and for "lowland" rivers (100-500 m) $c = 8$
331 and $d = -0.34$ (Milliman and Syvitski 1992). The values of the exponent d for the Hudson (-0.38 to -0.71)
332 are similar to the global values, but the leading coefficients c in the Hudson results (2.7 to 4.3) are less
333 than the global fits, reflecting the relatively low sediment yield for the U.S. Northeast in general (Meade
334 1969). These regressions specific to the Hudson allow estimation of the sediment yield on ungauged
335 tributaries, and provide better context for the background sediment load in assessing potential impacts of
336 dam removals.

337 Gauged rivers discharging into the tidal Hudson represent about 80% of the total watershed area, allowing
338 for direct calculation of most of the sediment input to the estuary (Table 1). For these gauged tributaries,
339 the total sediment load averaged about 1.1 Mt yr^{-1}, based directly on the sediment discharge
340 measurements or calculated from the discharge regressions. The total sediment load calculated using the
341 regressions with the full discharge records is slightly lower at 1.0 Mt yr^{-1}, in large part because the long-
342 term (~100 yr) discharges from the Mohawk and Upper Hudson are lower than the recent period when
343 most of the sediment measurements were made. The more recent, higher sediment load estimates are
344 potentially more relevant, as they are consistent with observations that the region is getting wetter
345 (Armstrong et al. 2014) and yielding more sediment (Cook et al. 2015). If we use watershed area to
346 proportionally scale the gauged inputs to the tidal river above Poughkeepsie (112 rkm) the annual
347 sediment load is 1.2 Mt yr^{-1}. The additional sediment input seaward of that is minimal due to the small
348 watershed area and low sediment yield (described below, Table 1). This result is greater than previous
349 estimates of sediment input to the Hudson. Observations in the tidal river along with the Mohawk and
350 Upper Hudson sediment discharge were used to find an average of 0.7 Mt yr^{-1} input to the tidal river
351 above Poughkeepsie for the period 2002-2006 (Wall et al. 2008). Previous observations in the estuary
352 found sediment inputs of 0.7 Mt yr^{-1} above Poughkeepsie and 1.1 Mt yr^{-1} above The Battery in 1959-1960
353 and 1977 respectively (Panuzio 1965; Olsen 1979), and watershed modeling was used to estimate 0.4-0.5
354 Mt yr^{-1} to the estuary for 1984-1986 (Swaney et al. 1996), a period with lower than average discharge
355 (Wall et al. 2008).

4.2 Sediment trapped in impoundments

357 Sediment masses in the 17 studied impoundments ranged from 5.9 Mt in Ashokan Reservoir built in 1915
358 and New York City's second largest public water supply reservoir, to 430 t in Hand Hollow Pond, a small
359 recreation pond built in 1980 with a contributing watershed area of 0.34 km^2 drained by a perennial inlet
360 stream. From a detailed analysis of the 97 dams in the Stockport Creek watershed (Fig. 1), which includes
361 Kinderhook Creek, we determined surprisingly that only 4 sites were active sediment traps, with the
362 remainder of the sites falling into categories run-of-river (23) and non-sources of sediment (70) consisting
363 of naturally breached dams, spring-fed impoundments, and dammed natural lakes. This important finding

364   was not expected and serves to highlight that the extensive distribution of inventoried dams mapped
365   within the Hudson watershed does not necessary reflect equally widespread and enhanced trapping of
366   sediment behind them. Total trapped sediment in the Stockport Creek watershed amounted to 0.36 Mt,
367   with the four active traps comprising 0.14 Mt, of which roughly 80% comes from one site (Summit Lake,
368   54 km^2 watershed). Run-of-river sites contained the remainder of the sediment that could be mobilized via
369   dam removal. Poor data quality in the NID database for small upland sites, including missing dam ages,
370   missing watershed sizes, and missing dam heights makes their evaluation difficult. The total sediment
371   inventory at these sites is likely small as stock ponds and recreation ponds typically take advantage of
372   groundwater springs where inputs of surface water and sediment are small.

373   Impoundments in the other study watersheds adjacent to Tivoli and Iona Island marshes were similarly
374   categorized, and trapped sediment masses were calculated based on impoundment size characteristics
375   from the NID database (Table 3). The Tivoli watersheds (Esopus, Saw Kill, and Stoney Creek) represent
376   a similar area as Stockport and have about half as many dams (52), but the impounded sediment mass is
377   about 0.64 Mt, almost twice that in Stockport. Sediment stored within Ashokan Reservoir was not
378   included in this value, as it is unlikely to be removed given its importance as a public water supply. The
379   Esopus watershed drains the Catskill Mountains, which as noted above have greater sediment yields than
380   the Taconic range on the east side of the Hudson, where the Stockport watershed is. The Iona watershed is
381   smaller and has fewer dams (33), and the sediment mass trapped is a factor of 10 or more less than the
382   other watersheds.

383   We scale up this detailed assessment of the sediment mass trapped in the three study watersheds to the
384   entire lower Hudson watershed. The study region lies predominantly within four physiographic provinces
385   (Fenneman and Johnson, 1946): Taconic, Catskill, Hudson Highlands, and Hudson Lowlands. We apply
386   the trapped sediment masses per unit watershed area from the study watersheds to the corresponding
387   physiographic province (Stockport for Taconic, Tivoli for Catskill, and Iona for Hudson Highlands), and
388   use total areas of each province in the Lower Hudson watershed (i.e. below Troy, Fig. 1), to estimate total
389   trapped mass (Table 4). Only a few of the study impoundments were located in the Hudson Lowlands
390   province, so we assumed an intermediate value for the trapped sediment mass per watershed area of 100 t
391   km^{-2}, between the Hudson Highland and Taconic values. Summing across the four provinces, we estimate
392   about 3.1 Mt of impounded sediment for the Lower Hudson watershed, excluding storage within two
393   aforementioned public water supply reservoirs, Ashokan and Rondout. This total is less than the 5.9 Mt
394   impounded sediment mass estimated for the Ashokan Reservoir, which is the largest impoundment in the
395   Lower Hudson, but it provides a useful estimate for the potential for sediment release from the numerous
396   smaller dams in the watershed. This also represents about 3 times the total average annual sediment input
397   to the Lower Hudson (Table 1).

398   Similarly, we can compare the total trapped sediment in each of the study watersheds to the typical
399   sediment supply from that watershed. Typical watershed sediment yields for Stockport (60 t km^{-2} yr^{-1}) and
400   Tivoli (100 t km^{-2} yr^{-1}) were determined based on the calculations from the sediment discharge
401   monitoring data (Table 1, Fig. 4). No water column-based sediment discharge measurements were
402   available for the Iona watershed. However, two of our impoundment sites (Nawahunta and Cortlandt)
403   within the watershed are efficient sediment traps, with Brune (1953) estimates of 58% and 71% of
404   incoming sediment trapped within these respective ponds. Based on the age of each dam, the mass of
405   sediment accumulated since construction, and accounting for sediment that flowed through each
406   impoundment without being trapped, we calculate sediment yields for these upstream watersheds of 6 and
407   11 t km^2 yr^{-1}. These low sediment yield estimates are consistent with the geologic characteristics of the
408   Hudson Highlands, where predominantly thin, rocky soils overlie erosion resistant crystalline rock.

409 Sediment yield estimates from the Housatonic and Connecticut River watersheds, which are east of the
410 lower Hudson and contain more micaceous rocks which tend to form finer textured soils, range between 8
411 and 30 t km^{-2} yr^{-1} (Yellen et al. 2014). Based on these observations and acknowledging uncertainty
412 derived from the small number of observations, we assumed a representative value of 10 t km^{-2} yr^{-1} for
413 Iona. Despite the low sediment yield, we estimate that the Hudson Highlands province likely stores a
414 similar percentage of sediment to Tivoli due to the high density of large and old (> 100 yrs) recreation
415 impoundments within large conserved parcels in the region. When combined, our total impounded
416 sediment mass in the study watersheds is estimated to represent on average 5-7 years of direct watershed
417 sediment supply to lower Hudson (excluding sources above Troy, NY, Fig. 1). This is greater than the
418 factor of 3 noted above for comparing the impounded sediment mass in the lower Hudson watershed to
419 the total annual sediment inputs because about half of the total watershed sediment supply comes from the
420 Mohawk and Upper Hudson (Table 1), where impounded sediment masses were not assessed.

421 In addition to the comparison of impounded sediment mass to sediment supply at the watershed scale, we
422 can use the sediment yield regressions (Fig. 4, Table 2) to make similar comparisons for individual
423 impoundments. Grant and Lewis (2015) defined the ratio of the mass of sediment that would be released
424 by a dam removal to the annual watershed sediment supply as the unitless term $E*$:

425 $$E^* = \frac{F_r M_r}{M_a} \qquad (2)$$

426 where M_r is the mass of sediment stored in the reservoir, F_r is the fraction of impounded sediment eroded
427 in the first year after dam removal, and M_a is the mass of sediment exported from the watershed annually.
428 The downstream impacts of sediment in tributaries was found to increase with this ratio, and in particular
429 the transport distance for coarse grained (sand and gravel) sediment (Grant and Lewis 2015). The
430 transport and deposition of finer grained sediment in tributaries was less directly linked to $E*$, but it
431 provides a useful metric for assessing potential impacts across spatial scales of watersheds and
432 impoundments. For each of the impoundments surveyed, watershed sediment discharge was calculated
433 based on the regressions of sediment yield vs. watershed area (Fig. 4, Table 2). The fraction of
434 impounded sediment eroded depends on factors such as grain size, impoundment geometry, and dam
435 removal method (Grant and Lewis 2015; Foley et al. 2017). We chose a typical value of $F_r = 0.5$, or about
436 half of the impounded sediment is eroded in the first year after removal, and the rest is stabilized in place
437 or is eroded in subsequent years. The $F_r = 0.5$ is likely an upper bound for sediment delivery to the
438 estuary, since impounded sediment that is not in-line with the impounded waterway is likely to be
439 sequestered in place, and deposition in the tributary or impoundments downstream from the dam removal
440 site would further reduce the fraction of impounded sediment reaching the estuary. $E*$ is plotted against
441 impoundment area, and generally has an increasing trend. Most of the $E*$ values are less than 1, indicating
442 that the sediment release from most of the impoundments would be less than the annual sediment load
443 from their local watershed (Fig. 5).

4.3 Grain size in impoundments and marshes

445 In addition to the mass of sediment in impoundments, sediment composition is a key factor in potential
446 impacts to the estuary. Sediment cores from impoundments were analyzed to characterize the particle size
447 distributions that might be mobilized following dam removals (Fig. 6). In most impoundments, the
448 median particle sizes (d_{50}) were fine silt, around 10-20 μm. The lower ends of the distributions
449 (represented by d_{10}) generally were clay-sized, whereas the upper limits (d_{90}) ranged from coarse silt to
450 medium sand. Cores were sampled at 10 cm intervals, but the particle size characteristics were relatively

451 uniform with depth. Grain size varied more between impoundments than between cores within an
452 impoundment, so only average values of d_{10}, d_{50}, and d_{90} for each impoundment are shown.

453 To assess the relevance of impounded sediment to wetland accretion in the estuary we need to consider
454 the particle size distributions in both the source and sink regions. Cores from tidal wetlands along the
455 Hudson were also subsampled at 10 cm intervals and analyzed for particle size (Fig. 6) (see also Yellen et
456 al., submitted). Median grain size in the marsh cores ranged from 10 to 25 μm, and lower and upper
457 bounds (d_{10} to d_{90}) were clay (2-4 μm) and very fine sand (70-100 μm), with the d_{90} potentially due to
458 incorporation of basal material. The strong similarities in particle size between the impoundments and
459 marshes suggest that sediment released to the estuary by dam removals could end up depositing in the
460 marshes and contribute to accretion.

461 Particle size determines settling velocity and thereby plays a dominant role in sediment transport and
462 deposition in the estuary. For individual particles, settling velocity can be related to particle diameter
463 based on a modified Stokes velocity (Dietrich 1982). This does not account for aggregation of smaller
464 particles into flocs that can increase their effective settling velocity. The assumption of discrete particle
465 settling is reasonable for sediment input to the freshwater tidal river and relatively short transport time
466 scales of weeks to months, but flocculation becomes a more significant factor in the saline estuary and at
467 longer time scales. For the modeling cases discussed in the next section, sediment classes with settling
468 velocities of 0.02, 0.2, 2.0 mm s^{-1} were used in dam removal release scenarios. These sediment classes
469 nominally correspond with clay (~7 μm), fine silt (~20 μm), and coarse silt (~60 μm), based on the
470 particle sizes in the impoundment cores (Fig. 6).

471 *4.4 Impacts of simulated dam releases in model results*

472 To quantify how sediment released after dam removal affects SSC and deposition in the estuary, realistic
473 model scenarios were run with increased sediment inputs from one of the tributaries. The results
474 presented here are for a simulation from spring and summer 2014 (Ralston and Geyer 2017). Total
475 discharge into the estuary increased rapidly to about 2500 m^3 s^{-1} at the end of March and then again to
476 2700 m^3 s^{-1} in mid-April (Fig. 7). Observed suspended sediment concentrations increased during the high
477 discharge periods, particularly in the upper tidal river, and then decreased through the summer. SSC
478 varied with tidal resuspension over the spring-neap cycle, particularly in the more seaward regions.

479 For the simulation shown in Fig. 7 the dam removal sediment input was from Kinderhook Creek near
480 Stockport marsh (188 rkm, $Q_{r,avg} = 16$ m^3 s^{-1}). The initial discharge event had a peak in Kinderhook of
481 about 200 m^3 s^{-1}, whereas a second event was smaller, around 70 m^3 s^{-1} (Fig. 7b). Q_s in the tributary
482 increases strongly with Q_r (Fig. 3e), so maximum SSC in the tributary during the first discharge event
483 was about 6 times greater than the second, and the first event had a much greater impact on SSC in the
484 estuary. For example, 13 km seaward of the input, SSC from the dam release sediment during the first
485 event was similar to that from all other sources, effectively doubling the concentration (Fig. 7c). During
486 the second event, and subsequently through most of the rest of the simulation, the dam sediment
487 concentrations were minimal compared to the total SSC at this nearest location. Brief increases in SSC at
488 this location due to the dam release also occurred during smaller discharge events in late spring and
489 summer, particularly for an event in the end of July (day 177) that had about 100 m^{3}s^{-1} compared to the
490 550 m^{3}s^{-1} from other tributaries. The SSC due to the dam release during this summer discharge event was
491 similar to that from other sources (resuspension and other tributaries), but the total SSC was much less
492 than during the freshet.

493   Farther seaward from the source tributary, the contribution of the dam release to the total SSC decreases.
494   At 36 km seaward, or several tidal excursions, dam sediment input approximately doubled the SSC during
495   the first discharge event, but for only several days (Fig. 7d). After that, dam release sediment did not
496   significantly contribute to the total SSC in the estuary. Farther downstream (91 km from the input), the
497   simulated dam release was barely perceptible, with background tidal resuspension far outweighing the
498   effects of increased upstream loading from the source tributary (Fig. 7e). Note that the background
499   sediment concentrations (and y-axis ranges in Fig. 7) vary among the selected locations depending on
500   local bed composition and sediment resuspension.

501   The total sediment input over the 5-month simulated release from dam removal in Stockport watershed
502   (Fig. 7) was about 45 kt. For comparison, the total sediment trapped behind 97 dams in the watershed was
503   estimated at 370 kt (Table 3), of which about half could potentially be mobilized and transported
504   downstream by dam removal (Grant and Lewis 2015; Foley et al. 2017). The largest impoundment in the
505   watershed, Summit Lake, has a trapped sediment mass of about 120 kt, so assuming a release fraction of
506   about 50%, the simulated dam release represents potential impacts on the estuary from one of the larger
507   sediment sources in the watershed. SSC in the estuary approximately doubled compared to background
508   for periods of a few days, but only during discharge events that affected primarily the local watershed and
509   only for regions within about a tidal excursion of the source. Details of the SSC impacts varied for the
510   other realistic simulation periods depending on the discharge and tidal forcing, but the magnitude and
511   extent of the effects were similar.

512   The seaward advection of the sediment pulse and decrease in SSC due to deposition of sediment from the
513   dam release was consistent with previous observations and modeling results (Ralston and Geyer 2017).
514   Sediment transport rates in the tidal river depend strongly on settling velocity, with coarser sediment
515   moving seaward more slowly and depositing closer to the input location (Ralston and Geyer 2017). The
516   particle size distributions in the impoundments ranged from clays to coarse silt, so the sediment inputs for
517   the dam removal were divided among three size classes by assuming a representative distribution: 15%
518   coarse silt (w_s = 2 mm s^{-1}), 40% fine silt (w_s = 0.2 mm s^{-1}), and 45% clay (w_s = 0.02 mm s^{-1}).

519   The settling velocity, or particle size, had a strong effect on the distance over which dam removal
520   sediment deposited in the estuary (Fig. 8). In all three of the tributary input locations that were simulated
521   (Stockport, Tivoli, and Iona), the coarse silt fraction deposited primarily within 10-20 km of the input.
522   The along-estuary structure of the deposition varied among the three cases due to local differences in the
523   bathymetry and the decreasing seaward transport rates in the wide lower reaches of the estuary, but the
524   deposition patterns depended more on settling velocity than input location. The fine silt class moved
525   farther seaward than the coarse silt, depositing up to 50-100 km from the source. The clay fraction
526   deposited even more broadly and uniformly, including into the lower reaches of the estuary.

527   Results from the 3-d model can be simplified to an algebraic expression relating seaward sediment
528   transport along the tidal river to channel geometry, river discharge and sediment settling velocity (Ralston
529   and Geyer 2017). This simplified approach allows for scaling of the distance away from the source
530   tributary of potential impacts by dam removals, and without the need for more detailed 3-d estuarine
531   simulations. The simplified model balances sediment advection and loss to deposition, with concentration
532   downstream from the input $C(x)$ depending on the input C_0, settling velocity w_s, water depth H_s, and an
533   advective time scale t_{adv} due to the mean river velocity, $U_0 = Q_r/A$ where A is the cross-sectional area:

534                  $$\frac{C(x)}{C_0} = \exp(-f\,\frac{w_s}{H_s}t_{adv}) \qquad\qquad (3)$$

535 This is based on Eqn. (4) from Ralston and Geyer (2017), but we combined their scaling factors into the
536 coefficient $f = 1/10$. We can rewrite this in terms of an advective length scale $L_{adv} = U_0 t_{adv}$, and relate it to
537 the decrease in sediment concentration relative to the input concentration:

538 $$L_{adv} = -10 \ln\left(\frac{C(x)}{C_0}\right)\frac{U_0 H_s}{w_s} \qquad (4)$$

539 The depth H_s represents the average depth of the shoals where settling predominantly occurs, and that
540 increases from about 5 m in the upper tidal river to about 12 m in the saline estuary (Fig. 13 of Ralston
541 and Geyer 2017). Using representative values for the input locations, we calculate L_{adv} for each settling
542 velocity by using the average river discharge ($\approx 600 \text{ m}^3 \text{s}^{-1}$) over the simulation period to get an average
543 U_0. As with the depth of the shoals, the cross-sectional area generally increases with distance seaward, so
544 the effective U_0 also depends on the release location (Table 5).

545 The advective lengths resulting from this scaling approach for $C/C_0 = 0.05$ are plotted as triangles in
546 Figure 8, representing the distance along the estuary where 95% of coarse silt and fine silt originating
547 from a dam release would deposit. The advective length scales are consistent with results from 3-d model
548 simulations. Coarse silt deposits within about 10 km of the releases in the upper tidal river, and within
549 half that distance for the Iona release location where the cross-sectional area is greater and U_0 less. In
550 Eqn. (4), L_{adv} scales inversely and linearly with settling velocity, resulting in length scales of about 100
551 km and 50 km respectively for fine silt from the upper and lower estuary inputs. The advective length
552 scales for the clay size class are greater than the length of the estuary, consistent with the results from the
553 3-d model showing transport and deposition throughout the estuary (Figure 8). The conceptual basis for
554 this simplified model falls apart in the saline estuary where the sediment transport and deposition patterns
555 also depend strongly on density-driven circulation, and so it is not applicable in the lower ~50 km.
556 However, the general correspondence between the advective length scale and sediment deposition for
557 coarse and fine silt suggests that the simplified approach can be used to scale the influence of sediment
558 from dam removals in the tidal river.

559 **5. Discussion**

560 *5.1 Estuarine impacts of sediment releases from dam removals*

561 The increase in sediment supply due to tributary dam releases can have either negative or positive impacts
562 on a downstream estuary. Negative impacts include decreases in water clarity or high rates of sediment
563 accretion that affect submerged vegetation (Hamberg et al. 2017; Glover et al. 2019) or lead to shifts in
564 ecosystem community composition (Cloern et al. 2007; Rubin et al. 2017). On the positive side, increases
565 in sediment supply might help tidal marshes keep up with sea level rise or reduce shoreline erosion rates
566 (Warrick et al. 2019). The results here indicate that for dam releases in the Hudson estuary, neither
567 positive nor negative impacts are expected to be pronounced. The Hudson has relatively high background
568 suspended sediment concentrations, from 50-100 mg/L in much of the tidal river and several hundred
569 mg/L or more in the saline estuary. During discharge events, direct watershed inputs can significantly
570 increase suspended sediment concentrations, particularly in the tidal river (Wall et al. 2008; Ralston and
571 Geyer 2017). During low to moderate flow periods in the tidal river, and more generally in the saline
572 estuary, resuspension of bed sediment by tidal currents is the dominant source of material in the water
573 column. This mobile pool of bed sediment available for resuspension gets redistributed throughout the
574 estuary, and can be many times greater mass than the annual input from the watershed (Schoellhamer
575 2011; Geyer and Ralston 2018). To significantly alter the sediment mass of the mobile pool and affect
576 turbidity in the estuary for months to years, any increase in sediment loading from dam removals would
577 have to be much greater than the mean annual input from the watershed or else sustained over many years

14

578 (Schoellhamer et al. 2013). We calculate that the total mass of impounded sediment within tributaries to
579 the Lower Hudson is similar to about 3 years of average sediment supply from the entire Hudson River.
580 As a likely upper constraint, we estimate that only about half the impounded sediment is likely to be
581 mobilized and transported downstream by dam removals. Furthermore, some of that released sediment
582 will be trapped in tributaries or by dams that are farther downstream. Last, sediment is likely to be
583 distributed among many impoundments and so is unlikely to be released in a short period. Given the
584 relatively small amount of sediment stored in impoundments and these mitigating factors, the potential
585 impacts of impounded sediment release on the mobile pool in the estuary are small.

586 The increase in sediment loading from one or more dam removals is analogous to the increased loading
587 from to the estuary during extreme discharge events. While the watershed sediment loads calculated
588 based on discharge regressions are meaningful as long-term averages, individual discharge events can
589 deliver many times the annual average over a few days. An example is from 2011, when tropical cyclones
590 Irene and Lee produced high precipitation, discharge, and sediment delivery to many estuaries in the U.S.
591 Northeast. The sediment load from the storms to the Delaware Estuary was similar to its annual average
592 (Sommerfield et al. 2017), and the Connecticut River estuary had sediment input of twice its annual
593 average over just 3 days (Yellen et al. 2014). In the Hudson, the sediment input from the storms was 2.7
594 Mt (Ralston et al. 2013), or about 3 times the annual average and similar to the total mass of sediment
595 stored in impoundments. Observations at multiple locations along the tidal river and saline estuary
596 showed increased turbidity during and in the months after the event (Ralston et al. 2013). Over the longer
597 term of the observational record (12 years), turbidity-discharge relationships in the tidal river increased on
598 average by 20 to 50% for up to 2 years after the events, but subsequently conditions returned to the long-
599 term averages (Ralston et al., submitted). This response was coherent across multiple stations in the tidal
600 river, but was not seen in the saline estuary, where background sediment concentrations and the size of
601 the mobile sediment pool are greater. The relatively modest increase in turbidity in the tidal river and
602 negligible impact on saline estuary from the extreme 2011 discharge events with 2.7 Mt of sediment input
603 corroborate the conclusions that the potential impacts of the total impounded sediment mass of 3.1 Mt
604 would also be modest, even in the unlikely scenario that it was all released to the estuary over a brief
605 period.

606 The increased sediment loading from dam removal could have more short-term or local impacts near the
607 source tributaries. The Hudson model results here as well as observations from the Elwha (Gelfenbaum et
608 al. 2015) indicate that even with relatively strong tidal currents, much of the coarser fraction from a dam
609 release deposits within a few km of the source. Dispersal along the estuary depends strongly on settling
610 velocity, with fine silt typically depositing within 50-100 km of the source and the clay-sized particles,
611 which make up more than 1/3 of the mass in many of the impoundments, dispersing throughout the
612 system. At the limit of the salinity intrusion, clay-sized particles would aggregate into flocs, increasing
613 their effective settling velocity and retention in the estuary (Geyer et al. 2001; Burchard et al. 2018).
614 Sediment accumulating in wetlands consists primarily of silt-sized particles (e.g., Fig. 6b), and these
615 results indicate that the fine sediment from dam releases deposits relatively far from the source rather than
616 primarily in local marshes. The advective distance scales with discharge so releases during low discharge
617 periods would be more likely to deposit near the source tributary. However, the relatively high
618 background SSC and marginal increases from the simulated releases suggest that effects on wetland
619 accretion rates in the Hudson would be small. Observations of accretion in the study marshes indicate that
620 the current rates of accretion are much greater than sea level rise, even without potential contributions
621 from dam removals (Yellen et al., submitted).

15

The dam removal impacts on sediment dynamics might be more significant in an estuary with a smaller mobile sediment pool and lower background concentrations. For example, the Connecticut River is the next major watershed to the east, and it has a similar mean discharge and sediment load as the Hudson (Woodruff et al. 2013). However, suspended sediment concentrations in the Connecticut River estuary are much lower than in the Hudson and the bed is predominantly sand rather than mud, even in the saline estuary (Patton and Horne 1992; Yellen et al. 2017). Dam removal inputs that were a significant fraction of the watershed input, particularly during lower discharge periods, might have a greater impact on this type of estuary that has less background sediment availability. Expansive salt marshes are located near the mouth of the Connecticut despite the relatively low background sediment concentrations, so increases in supply from dam removal may have proportionally greater impacts on accretion than along the tidal Hudson. Analogously, sediment supply limitations appear to be contributing to deterioration of the marshes near the mouth of the Hudson in Jamaica Bay (Peteet et al. 2018; Chant et al. submitted), so these coastal marshes could potentially benefit from increased sediment loading to the Hudson as a whole.

5.2 Watershed sediment inputs

Sediment input to the Hudson River estuary is highly variable at multiple time scales, and the sediment discharge regressions did not address this temporal variability. Precipitation events increase volumetric discharge in a tributary, but the resulting sediment load may depend on the spatial distribution and intensity of precipitation within the basin. Similarly, for a given Q_r the sediment discharge can depend on the antecedent conditions, with greater soil moisture due to prior events or seasonal differences leading to greater sediment yield (Yellen et al. 2016). Climate-driven changes in mean annual precipitation can lead to similar increases in soil moisture and sediment yield at decadal time scales (Cook et al. 2015), as can shifts in watershed land use (Schoellhamer et al. 2013; Warrick et al. 2013). Major discharge events can increase sediment availability in a watershed and thus increase sediment discharge for a given Q_r for several years, and this is typically followed by a longer period of lower than average sediment concentrations (Warrick et al. 2013; Gray 2018). Temporal variations in the relationship between Q_s and Q_r at event, annual, or decadal time scales can be addressed in some cases by subdividing the data or using dynamic linear models (Warrick et al. 2013; Ahn et al. 2017). For most of the gauging stations in this study the sediment discharge records were too short (< 5 years) to robustly assess temporal trends.

The total sediment load to the estuary of 1.2 Mt yr^{-1} based on the sediment-discharge regressions is greater than most values that have been reported previously. Many estimates of sediment load have been hampered by short data records and the intermittency of discharge events, or have focused on the two largest tributaries, the Upper Hudson and Mohawk. Here we used long-term discharge and sediment data covering about 80% of the watershed area. One long-term study quantified sediment inputs to the Hudson from the Upper Hudson and Mohawk over a 4 year period (2002-2006), and also measured net seaward sediment transport in the tidal river at Poughkeepsie, about midway between the head of tides and the mouth (Wall et al. 2008). During that period, the annual input from the Upper Hudson and Mohawk ranged between 0.37 and 0.89 Mt, whereas seaward transport in the tidal river varied from 0.68 and 0.83 Mt. Based on the difference between these measurements as well as the timing of sediment pulses from discharge events, the sediment load from smaller watersheds downstream of the Upper Hudson and Mohawk was estimated to be 30-40% of the total at Poughkeepsie, or about 0.26 Mt on average. From our stream gauge regressions, the sediment input below the tidal limit was 0.53 Mt, or about twice the previous value. A key unknown in the approach based on transport in the tidal river is the rate of sediment storage and accumulation landward of Poughkeepsie, which may contribute to the greater estimate from the watershed inputs. Yellen et al. (submitted) estimates that 0.07 Mt of sediment are stored annually in tidal flats and marshes within this reach, accounting for some of the discrepancy between sediment

16

667 delivery to the estuary and that which is transported past Poughkeepsie. Uncertainty due to discharge
668 variability also contributes to both estimates. Many of the gauges in smaller watersheds were operational
669 primarily after extreme discharge events from Tropical Storms Irene and Lee in 2011, which may have
670 influenced the sediment regressions or altered the watershed yields compared to the period of the earlier
671 study that had a more typical discharge range.

672 Uncertainty in the sediment loading to the estuary has broader implications than just for dam removal, as
673 it relates to contaminant transport (e.g., PCB loading from the Upper Hudson (Feng et al. 1998)), marsh
674 resilience, and frequency of dredging for navigation. Because of the nonlinear relationship between Q_r
675 and Q_s, uncertainty related to not accounting for temporal variability can lead to significant errors. For
676 example, using a single regression spanning 30 years for the Eel River (CA) would over-predict the
677 sediment load by a factor of 2.5 compared to including temporal variations because of changes in land use
678 and a record discharge event (Warrick et al. 2013). The most effective way to reduce the uncertainty is to
679 collect more sediment discharge monitoring data, and to link that with development of better models of
680 watershed hydrologic and geomorphic processes. This analysis provides a template and a more thorough
681 assessment of present conditions in the Hudson watershed, but assessing temporal trends with increases in
682 discharge due to climate change (Hayhoe et al. 2007) or alterations to land use will be difficult given that
683 sediment discharge measurements have been halted at many of the gauging stations.

684 **6. Summary**

685 Interest in dam removals is increasing to meet various objectives including improving aquatic
686 connectivity and removing safety hazards. Dam removals often result in mobilization and transport
687 downstream of sediment that had previously been trapped in the impoundment. Potential impacts of this
688 sediment release on ecosystems and geomorphology in the fluvial reaches downstream of dams are being
689 examined more widely, but effects of that sediment on estuaries and coastal regions that are farther
690 seaward have received less attention. Increased sediment loading to an estuary can have negative impacts
691 through increased turbidity causing decreased light availability or through changes to benthic habitat by
692 increased deposition rates, but it can also potentially be a net benefit for supplying sediment to wetlands
693 that can increase resilience to sea level rise. We used a combination of observational and modeling
694 approaches to characterize potential impacts of sediment released from dam removals in the Hudson
695 River estuary, including quantification of watershed sediment loading for comparison and assessment of
696 the magnitude and extent of impacts in the estuary.

697 Using volumetric and sediment discharge data from 11 stations we developed sediment-discharge
698 regressions and calculate average sediment loads for tributaries that account for about 80% of the
699 watershed area for the Hudson River Estuary, and about 90% of the watershed discharging to the tidal
700 river (Fig. 3). The total average input is about 1.2 Mt, of which about 45% comes from smaller
701 watersheds that discharge seaward of the head of tides. Watershed sediment yields vary inversely with
702 watershed area in a manner similar to regressions based on global rivers (Fig. 4). In addition, sediment
703 yields depend on regional variations in lithology, with greater yields for watershed draining the more
704 erodible and finer textured soils of the Catskill Mountains to the west of the Hudson than those sandier
705 soils in the watersheds in the Taconic Mountains to the east. The regressions allow for estimation of
706 sediment yield for ungauged subwatersheds of the estuary, which can provide context for potential
707 impacts of sediment released by a dam removal in subwatersheds.

708 Geophysical surveys of 17 impoundments in five subwatersheds of the Hudson estuary were used to
709 evaluate the mass and composition of sediment trapped behind dams. The surveyed impoundments were
710 grouped into three functional categories: 1. active sediment traps, 2. run-of-river sites with impounded

17

711 sediment but that were no longer trapping, and 3. dams on natural lakes or springs that did not
712 significantly alter sediment delivery. A vast majority of the 1700 dams within the Hudson watershed
713 inventory are assessed as the latter two categories and as such are not currently increasing sediment
714 trapping in the watershed. Impounded sediment mass was calculated from cores and spatial surveys at the
715 study sites, and these results along with the federal dam database were used to estimate a total impounded
716 sediment mass of 3.1 Mt in the watershed of the Lower Hudson. From other studies, about half of the
717 sediment behind an impoundment is released with dam removal (Grant and Lewis 2015; Foley et al.
718 2017). This suggests that the total mass of sediment that could potentially be released from the
719 approximately 1700 impoundments represents less than 2 years of average watershed sediment input.
720 The watershed sediment yields are compared with sediment masses at the study sites to show that similar
721 results hold at the scale of individual impoundments (Fig. 5).

722 In addition to the broader scale impacts on the sediment budget for the entire estuary, sediment releases
723 from dam removals may have more localized or brief impacts near the input tributary. To assess impacts
724 along the estuary, we used a 3-d hydrodynamic and sediment transport model to simulate increased
725 sediment inputs representative of dam removal under realistic forcing conditions. The dam removal inputs
726 did increase suspended sediment concentrations, but only modestly during discharge events and within
727 about a tidal excursion of the input tributary (Fig. 7). The model results were sensitive to settling
728 velocities, which were determined based on particle size distributions in the impoundment cores (Fig. 6).
729 Coarse silt (w_s = 2 mm s^{-1}) typically deposited within 5-10 km of the source, whereas fine silt (0.2 mm s^{-1})
730 and clay (0.02 mm s^{-1}) dispersed more broadly along the estuary. The deposition patterns from the full 3-d
731 model were consistent with advective length scales from a simplified, 1-d approach that could be applied
732 more broadly. Particle size distributions from cores in tidal wetlands along the Hudson are more
733 consistent with these smaller size classes, suggesting that any potential impacts of increased sediment
734 delivery to the estuary from dam removal would be broadly distributed rather than restricted to the near
735 source. Currently sediment accretion rates along the tidal Hudson are similar to or greater than sea level
736 rise, even without sediment from dam removals. This, and the comparisons of impounded sediment mass
737 to watershed sediment loads suggest that the effects of sediment release from dam removal on the Hudson
738 would be modest. However, other estuaries with lower sediment loads, smaller mobile sediment pools, or
739 larger impoundments are more likely to be significantly affected.

References

746 Ahearn, Dylan S., and Randy A. Dahlgren. 2005. Sediment and nutrient dynamics following a low-head
747   dam removal at Murphy Creek, California. *Limnology and Oceanography* 50: 1752–1762.
748 Ahn, Kuk-Hyun, Brian Yellen, and Scott Steinschneider. 2017. Dynamic linear models to explore time-
749   varying suspended sediment-discharge rating curves. *Water Resources Research* 53: 4802–4820.
750 Armstrong, William H., Mathias J. Collins, and Noah P. Snyder. 2014. Hydroclimatic flood trends in the
751   northeastern United States and linkages with large-scale atmospheric circulation patterns.
752   *Hydrological Sciences Journal* 59: 1636–1655.
753 Avnimelech, Yoram, Gad Ritvo, Leon E. Meijer, and Malka Kochba. 2001. Water content, organic carbon
754   and dry bulk density in flooded sediments. *Aquacultural engineering* 25: 25–33.

Bowen, Melissa M., and W. Rockwell Geyer. 2003. Salt transport and the time-dependent salt balance of a partially stratified estuary. *Journal of Geophysical Research* 108: 3158. doi:10.1029/2001JC001231.

Brune, Gunnar M. 1953. Trap efficiency of reservoirs. *Eos, Transactions American Geophysical Union* 34: 407–418.

Burchard, Hans, Henk M. Schuttelaars, and David K. Ralston. 2018. Sediment Trapping in Estuaries. *Annual Review of Marine Science* 10: 371–395. doi:10.1146/annurev-marine-010816-060535.

Cleveland, William S. 1979. Robust locally weighted regression and smoothing scatterplots. *Journal of the American statistical association* 74: 829–836.

Cloern, James E., Alan D. Jassby, Janet K. Thompson, and Kathryn A. Hieb. 2007. A cold phase of the East Pacific triggers new phytoplankton blooms in San Francisco Bay. *Proceedings of the National Academy of Sciences* 104: 18561–18565. doi:10.1073/pnas.0706151104.

Cohn, T. A. 1995. Recent advances in statistical methods for the estimation of sediment and nutrient transport in rivers. *Reviews of Geophysics* 33: 1117–1123. doi:10.1029/95RG00292.

Collins, M. J., Noah P. Snyder, Graham Boardman, William SL Banks, Mary Andrews, Matthew E. Baker, Maricate Conlon, Allen Gellis, Serena McClain, and Andrew Miller. 2017. Channel response to sediment release: insights from a paired analysis of dam removal. *Earth Surface Processes and Landforms* 42: 1636–1651.

Cook, Timothy L., Brian C. Yellen, Jonathan D. Woodruff, and Daniel Miller. 2015. Contrasting human versus climatic impacts on erosion. *Geophysical Research Letters* 42: 6680–6687.

Dean, Walter E. 1974. Determination of carbonate and organic matter in calcareous sediments and sedimentary rocks by loss on ignition; comparison with other methods. *Journal of Sedimentary Research* 44: 242–248.

Dicken, Connie L., Suzanne W. Nicholson, John D. Horton, Scott A. Kinney, Gregory Gunther, Michael P. Fosse, and Julia A. L. Mueller. 2005. *Integrated Geologic Map Databases for the United States: Delaware, Maryland, New York, Pennsylvania, and Virginia*. Open-File Report 2005–1325. Reston, VA: U.S. Geological Survey.

Dietrich, William E. 1982. Settling velocity of natural particles. *Water Resources Research* 18: 1615–1626. doi:10.1029/WR018i006p01615.

Doyle, Martin W., Emily H. Stanley, and Jon M. Harbor. 2003. Channel adjustments following two dam removals in Wisconsin. *Water Resources Research* 39. doi:10.1029/2002WR001714.

Faber, Marjorie. 2002. Soil survey of Dutchess County, New York.

Feng, Huan, J. Kirk Cochran, Honoratha Lwiza, Bruce J. Brownawell, and David J. Hirschberg. 1998. Distribution of heavy metal and PCB contaminants in the sediments of an urban estuary: the Hudson River. *Marine environmental research* 45: 69–88.

Ferguson, R. I. 1986. River loads underestimated by rating curves. *Water resources research* 22: 74–76.

Foley, M. M., J. R. Bellmore, J. E. O'Connor, J. J. Duda, A. E. East, G. E. Grant, C. W. Anderson, et al. 2017. Dam removal: Listening in. *Water Resources Research* 53: 5229–5246. doi:10.1002/2017WR020457.

Ganju, Neil K. 2019. Marshes Are the New Beaches: Integrating Sediment Transport into Restoration Planning. *Estuaries and Coasts* 42: 917–926.

Ganju, Neil K., Nicholas J. Nidzieko, and Matthew L. Kirwan. 2013. Inferring tidal wetland stability from channel sediment fluxes: Observations and a conceptual model. *Journal of Geophysical Research: Earth Surface* 118: 2045–2058.

Gelfenbaum, Guy, Andrew W. Stevens, Ian Miller, Jonathan A. Warrick, Andrea S. Ogston, and Emily Eidam. 2015. Large-scale dam removal on the Elwha River, Washington, USA: Coastal geomorphic change. *Geomorphology* 246: 649–668.

802 Geyer, W. Rockwell, and D. K. Ralston. 2018. A mobile pool of contaminated sediment in the Penobscot
803   Estuary, Maine, USA. *Science of The Total Environment* 612: 694–707.
804   doi:10.1016/j.scitotenv.2017.07.195.
805 Geyer, W. Rockwell, Jonathan D. Woodruff, and Peter Traykovski. 2001. Sediment Transport and
806   Trapping in the Hudson River Estuary. *Estuaries* 24: 670–679.
807 Glover, H.E., A. S. Ogston, I. M. Miller, E. F. Eidam, S. P. Rubin, and H. D. Berry. 2019. Impacts of
808   Suspended Sediment on Nearshore Benthic Light Availability Following Dam Removal in a Small
809   Mountainous River: In Situ Observations and Statistical Modeling. *Estuaries and Coasts*.
810   doi:10.1007/s12237-019-00602-5.
811 Grant, Gordon E., and Sarah L. Lewis. 2015. The remains of the dam: what have we learned from 15
812   years of US dam removals? In *Engineering Geology for Society and Territory-Volume 3*, 31–35.
813   Springer.
814 Gray, Andrew B. 2018. The impact of persistent dynamics on suspended sediment load estimation.
815   *Geomorphology* 322: 132–147.
816 Hamberg, Jonas, Stuart E. G. Findlay, Karin E. Limburg, and Stewart A. W. Diemont. 2017. Post-storm
817   sediment burial and herbivory of Vallisneria americana in the Hudson River estuary: mechanisms
818   of loss and implications for restoration. *Restoration Ecology* 25: 629–639.
819   doi:10.1111/rec.12477.
820 Hayhoe, Katharine, Cameron P. Wake, Thomas G. Huntington, Lifeng Luo, Mark D. Schwartz, Justin
821   Sheffield, Eric Wood, et al. 2007. Past and future changes in climate and hydrological indicators
822   in the US Northeast. *Climate Dynamics* 28: 381–407. doi:10.1007/s00382-006-0187-8.
823 Helsel, Dennis R., and Robert M. Hirsch. 2002. *Statistical methods in water resources*. Vol. 323. US
824   Geological Survey Reston, VA.
825 Hicks, D. Murray, Basil Gomez, and Noel A. Trustrum. 2000. Erosion thresholds and suspended sediment
826   yields, Waipaoa River basin, New Zealand. *Water Resources Research* 36: 1129–1142.
827 Lerczak, James A., W. Rockwell Geyer, and Robert J. Chant. 2006. Mechanisms Driving the Time-
828   Dependent Salt Flux in a Partially Stratified Estuary. *Journal of Physical Oceanography* 36: 2296–
829   2311.
830 Magilligan, F. J., K. H. Nislow, B. E. Kynard, and A. M. Hackman. 2016. Immediate changes in stream
831   channel geomorphology, aquatic habitat, and fish assemblages following dam removal in a small
832   upland catchment. *Geomorphology* 252: 158–170.
833 Magirl, Christopher S., Robert C. Hilldale, Christopher A. Curran, Jeffrey J. Duda, Timothy D. Straub,
834   Marian Domanski, and James R. Foreman. 2015. Large-scale dam removal on the Elwha River,
835   Washington, USA: Fluvial sediment load. *Geomorphology* 246: 669–686.
836 Major, Jon J., Jim E. O'Connor, Charles J. Podolak, Mackenzie K. Keith, Gordon E. Grant, Kurt R. Spicer,
837   Smokey Pittman, Heather M. Bragg, J. Rose Wallick, and Dwight Q. Tanner. 2012. *Geomorphic*
838   *response of the Sandy River, Oregon, to removal of Marmot Dam*. US Department of the Interior,
839   US Geological Survey Washington, DC.
840 McHale, Michael R., and Jason Siemion. 2014. *Turbidity and suspended sediment in the upper Esopus*
841   *Creek watershed, Ulster County, New York*. Scientific Investigations Report 2014–5200. U.S.
842   Geological Survey.
843 Meade, Robert H. 1969. Landward transport of bottom sediments in estuaries of the Atlantic Coastal
844   Plain. *Journal of Sedimentary Petrology* 39: 222–234.
845 Milliman, John D., and James PM Syvitski. 1992. Geomorphic/tectonic control of sediment discharge to
846   the ocean: the importance of small mountainous rivers. *The journal of Geology* 100: 525–544.
847 Mukundan, Rajith, D. C. Pierson, E. M. Schneiderman, D. M. O'donnell, S. M. Pradhanang, M. S. Zion, and
848   A. H. Matonse. 2013. Factors affecting storm event turbidity in a New York City water supply
849   stream. *Catena* 107: 80–88.

850 Nash, D. B. 1994. Effective sediment-transporting discharge from magnitude-frequency analysis. *Journal*
851   *of Geology* 102: 79–96.
852 Nitsche, F.O., W.B.F. Ryan, S.M. Carbotte, R.E. Bell, A. Slagle, C. Bertinado, R. Flood, T. Kenna, and C.
853   McHugh. 2007. Regional patterns and local variations of sediment distribution in the Hudson
854   River Estuary. *Estuarine, Coastal and Shelf Science* 71: 259–277. doi:10.1016/j.ecss.2006.07.021.
855 O'Connor, J. E., J. J. Duda, and G. E. Grant. 2015. 1000 dams down and counting. *Science* 348: 496–497.
856   doi:10.1126/science.aaa9204.
857 Olsen, Curtis R. 1979. Radionuclides, sedimentation and the accumulation of pollutants in the Hudson
858   River Estuary. Ph.D., Columbia University.
859 Olsson, Karl S. 1981. *Soil survey of Orange County, New York*. Vol. 22. US Department of Agriculture, Soil
860   Conservation Service.
861 Orth, Robert J., and Kenneth A. Moore. 1984. Distribution and abundance of submerged aquatic
862   vegetation in Chesapeake Bay: An historical perspective. *Estuaries* 7: 531–540.
863   doi:10.2307/1352058.
864 Panuzio, F. L. 1965. Lower Hudson River siltation. In *Proceedings of the 2nd Federal Interagency*
865   *Sedimentation Conference*, 512–550. Misc. Publication 970. Jackson, MS: Agricultural Research
866   Service.
867 Patton, Peter C., and Gregory S. Horne. 1992. Response of the Connecticut River estuary to late
868   Holocene sea level rise. *Geomorphology* 5: 391–417.
869 Pearson, Adam J., Noah P. Snyder, and Mathias J. Collins. 2011. Rates and processes of channel response
870   to dam removal with a sand-filled impoundment. *Water Resources Research* 47: W08504.
871   doi:10.1029/2010WR009733.
872 Pennington, W., T. G. Tutin, R. S. Cambray, and E. M. Fisher. 1973. Observations on lake sediments using
873   fallout 137 Cs as a tracer. *Nature* 242: 324–326.
874 Peteet, Dorothy M., Jonathan Nichols, Timothy Kenna, Clara Chang, James Browne, Mohammad Reza,
875   Stephen Kovari, Louisa Liberman, and Stephanie Stern-Protz. 2018. Sediment starvation destroys
876   New York City marshes' resistance to sea level rise. *Proceedings of the National Academy of*
877   *Sciences* 115: 10281–10286.
878 Phillips, Patrick J., and Dorothea W. Hanchar. 1996. Water-quality assessment of the Hudson River Basin
879   in New York and adjacent states. *Water-Resources Investigations Report* 96: 4065.
880 Pizzuto, Jim. 2002. Effects of Dam Removal on River Form and Process: Although many well-established
881   concepts of fluvial geomorphology are relevant for evaluating the effects of dam removal,
882   geomorphologists remain unable to forecast stream channel changes caused by the removal of
883   specific dams. *BioScience* 52: 683–691.
884 Ralston, David K., and W. Rockwell Geyer. 2017. Sediment transport time scales and trapping efficiency
885   in a tidal river. *Journal of Geophysical Research: Earth Surface* 122: 2042–2063.
886 Ralston, David K., W. Rockwell Geyer, and James A. Lerczak. 2008. Subtidal Salinity and Velocity in the
887   Hudson River Estuary: Observations and Modeling. *Journal of Physical Oceanography* 38: 753–
888   770.
889 Ralston, David K., W. Rockwell Geyer, and John C. Warner. 2012. Bathymetric controls on sediment
890   transport in the Hudson River estuary: Lateral asymmetry and frontal trapping. *Journal of*
891   *Geophysical Research* 117: C10013. doi:10.1029/2012JC008124.
892 Ralston, David K., Stefan Talke, W. Rockwell Geyer, Hussein A. M. Al-Zubaidi, and Christopher K.
893   Sommerfield. 2019. Bigger Tides, Less Flooding: Effects of Dredging on Barotropic Dynamics in a
894   Highly Modified Estuary. *Journal of Geophysical Research: Oceans* 124: 196–211.
895   doi:10.1029/2018JC014313.

896   Ralston, David K., John C. Warner, W. Rockwell Geyer, and Gary R. Wall. 2013. Sediment transport due
897   to extreme events: The Hudson River estuary after tropical storms Irene and Lee. *Geophysical*
898   *Research Letters* 40: 2013GL057906. doi:10.1002/2013GL057906.
899   Ralston, David K., Brian Yellen, Jonathon D. Woodruff, Sarah Fernald. 2020 (submitted). Turbidity
900   hysteresis in an estuary and tidal river following an extreme discharge event, *Geophys. Res.*
901   *Letters.*, submitted Mar 2020.

902   Riggsbee, J. Adam, Jason P. Julian, Martin W. Doyle, and Robert G. Wetzel. 2007. Suspended sediment,
903   dissolved organic carbon, and dissolved nitrogen export during the dam removal process. *Water*
904   *Resources Research* 43. doi:10.1029/2006WR005318.
905   Rubin, Stephen P., Ian M. Miller, Melissa M. Foley, Helen D. Berry, Jeffrey J. Duda, Benjamin Hudson,
906   Nancy E. Elder, et al. 2017. Increased sediment load during a large-scale dam removal changes
907   nearshore subtidal communities. *PLOS ONE* 12: e0187742. doi:10.1371/journal.pone.0187742.
908   Sawaske, Spencer R., and David L. Freyberg. 2012. A comparison of past small dam removals in highly
909   sediment-impacted systems in the U.S. *Geomorphology* 151–152: 50–58.
910   doi:10.1016/j.geomorph.2012.01.013.
911   Schoellhamer, David H. 2011. Sudden Clearing of Estuarine Waters upon Crossing the Threshold from
912   Transport to Supply Regulation of Sediment Transport as an Erodible Sediment Pool is Depleted:
913   San Francisco Bay, 1999. *Estuaries and Coasts* 34: 885–899. doi:10.1007/s12237-011-9382-x.
914   Schoellhamer, David H., Scott A. Wright, and Judith Z. Drexler. 2013. Adjustment of the San Francisco
915   estuary and watershed to decreasing sediment supply in the 20th century. *Marine Geology* 345:
916   63–71.
917   Smith, S. M. C., and P. R. Wilcock. 2015. Upland sediment supply and its relation to watershed sediment
918   delivery in the contemporary mid-Atlantic Piedmont (USA). *Geomorphology* 232. Elsevier: 33–
919   46.
920   Sommerfield, Christopher K., Daniel I. Duval, and Robert J. Chant. 2017. Estuarine sedimentary response
921   to Atlantic tropical cyclones. *Marine Geology* 391: 65–75. doi:10.1016/j.margeo.2017.07.015.
922   Swaney, D. P., D. Sherman, and R. W. Howarth. 1996. Modeling Water, Sediment and Organic Carbon
923   Discharges in the Hudson-Mohawk Basin: Coupling to Terrestrial Sources. *Estuaries* 19: 833–847.
924   doi:10.2307/1352301.
925   Swaney, Dennis P., Karin E. Limburg, and Karen Stainbrook. 2006. Some historical changes in the
926   patterns of population and land use in the Hudson River watershed. In *American Fisheries*
927   *Society Symposium*, 51:75. American Fisheries Society.
928   Syvitski, James P., Mark D. Morehead, David B. Bahr, and Thierry Mulder. 2000. Estimating fluvial
929   sediment transport: The rating parameters. *Water Resources Research* 36: 2747–2760.
930   doi:10.1029/2000WR900133.
931   Tullos, Desirée D., Mathias J. Collins, J. Ryan Bellmore, Jennifer A. Bountry, Patrick J. Connolly, Patrick B.
932   Shafroth, and Andrew C. Wilcox. 2016. Synthesis of Common Management Concerns Associated
933   with Dam Removal. *JAWRA Journal of the American Water Resources Association* 52: 1179–
934   1206. doi:10.1111/1752-1688.12450.
935   Wall, G., E. Nystrom, and S. Litten. 2008. Suspended Sediment Transport in the Freshwater Reach of the
936   Hudson River Estuary in Eastern New York. *Estuaries and Coasts*. doi:10.1007/s12237-008-9050-
937   y.
938   Warner, John C., Brandy Armstrong, Ruoying He, and Joseph B. Zambon. 2010. Development of a
939   Coupled Ocean–Atmosphere–Wave–Sediment Transport (COAWST) Modeling System. *Ocean*
940   *Modelling* 35: 230–244. doi:10.1016/j.ocemod.2010.07.010.

941 Warrick, J. A., Mary Ann Madej, M. A. Goñi, and R. A. Wheatcroft. 2013. Trends in the suspended-
942   sediment yields of coastal rivers of northern California, 1955–2010. *Journal of hydrology* 489:
943   108–123.
944 Warrick, Jonathan A., Jennifer A. Bountry, Amy E. East, Christopher S. Magirl, Timothy J. Randle, Guy
945   Gelfenbaum, Andrew C. Ritchie, George R. Pess, Vivian Leung, and Jeffrey J. Duda. 2015. Large-
946   scale dam removal on the Elwha River, Washington, USA: Source-to-sink sediment budget and
947   synthesis. *Geomorphology* 246: 729–750.
948 Warrick, Jonathan A., Andrew W. Stevens, Ian M. Miller, Shawn R. Harrison, Andrew C. Ritchie, and Guy
949   Gelfenbaum. 2019. World's largest dam removal reverses coastal erosion. *Scientific Reports* 9:
950   1–12. doi:10.1038/s41598-019-50387-7.
951 Wilcox, Andrew C., Jim E. O'Connor, and Jon J. Major. 2014. Rapid reservoir erosion, hyperconcentrated
952   flow, and downstream deposition triggered by breaching of 38 m tall Condit Dam, White Salmon
953   River, Washington. *Journal of Geophysical Research: Earth Surface* 119: 1376–1394.
954   doi:10.1002/2013JF003073.
955 Woodruff, Jonathan D. 1999. Sediment deposition in the lower Hudson River estuary. M.S. thesis,
956   Massachussets Institute of Technology/Woods Hole Oceanographic Institution.
957 Woodruff, Jonathan D., Anna P. Martini, Emhmed ZH Elzidani, Thomas J. Naughton, Daniel J. Kekacs, and
958   Daniel G. MacDonald. 2013. Off-river waterbodies on tidal rivers: Human impact on rates of
959   infilling and the accumulation of pollutants. *Geomorphology* 184: 38–50.
960 Yellen, B., J. D. Woodruff, L. N. Kratz, S. B. Mabee, J. Morrison, and A. M. Martini. 2014. Source,
961   conveyance and fate of suspended sediments following Hurricane Irene. New England, USA.
962   *Geomorphology* 226: 124–134.
963 Yellen, Brian, Jonathan D. Woodruff, Timothy L. Cook, and Robert M. Newton. 2016. Historically
964   unprecedented erosion from Tropical Storm Irene due to high antecedent precipitation. *Earth
965   Surface Processes and Landforms* 41: 677–684. doi:10.1002/esp.3896.
966 Yellen, Brian, Jonathan D. Woodruff, David K. Ralston, D. G. MacDonald, and D. S. Jones. 2017. Salt
967   wedge dynamics lead to enhanced sediment trapping within side embayments in high-energy
968   estuaries. *Journal of Geophysical Research: Oceans*: n/a-n/a. doi:10.1002/2016JC012595.
969 Yellen, Brian, Jonathon D. Woodruff, Caroline Ladlow, David K. Ralston, Sarah Fernald, Waverly Lau.
970   2020 (submitted). Rapid Tidal Marsh Development in Anthropogenic Backwaters – Implications
971   for Marsh Creation and Restoration, *Geomorphology*, submitted Mar 2020.

972

973   **Tables**

	USGS station	Watershed area (km^2)	Q$_s$ obs.	Q$_r$ obs.	Mean discharge (Q$_r$) [m^3 s^{-1}]		Mean sediment load (Q$_s$) [kton yr^{-1}]			Yield (t km^{-2} yr^{-1})
					Q$_s$ obs	all Q$_r$	Obs.	Q$_r$ fit (Q$_s$ obs.)	Q$_r$ fit (all Q$_r$)	Q$_r$ fit (all Q$_r$)
a	Schoharie (01351500)	2295	2012-2015	1939-2019	29	32	131	124	300	131
b	Mohawk @ Cohoes (01357500)*	8935	1954-2018*	1917-2019	195	168	454	473	363	41
c	Upper Hudson @ Waterford (01335770)*	11955	1976-2014	1887-2016	249	223	191	153	148	12
d	Catskill (01362090)*	1049	2011-2015	2011-2015	21	21	221	267	267	254
e	Kinderhook (01361000)*	852	2011-2014	1906-2019	16	13	58	68	36	43
f	Roeliff Jansen (01362182)*	549	2011-2014	2011-2014	11	11	18	19	19	35
g	Rondout (01362182)*	3069	2011-2015	2011-2015	65	64	106	87	87	28
H	Stony Clove (01362370)	80	2011-2014	1997-2019	2	3	14	16	155	1930
I	Esopus @ Coldbrook (01362500)	497	2012-2019	1931-2019	22	21	48	46	99	199
J	Esopus @ Lomontville (01363556)	723	2013-2015	2013-2019	3	6	3	2	4	5
k	Esopus @ Mount Marion (01364500)*	1085	2013-2015	1907-2019	10	16	14	11	59	54
	Total discharging to tidal Hudson (*)	27494			567	516	1062	1078	979	36
	Seaward estimates scaled by watershed area									
	Poughkeepsie	30406			627	571	1174	1192	1083	36
	The Battery	34680			715	651	1217	1235	1125	32
	* discontinuous coverage: 1953-1959, 1976-1979, 2004-2018									

974

975   **Table 1.** Mean discharge (Q$_r$) and sediment load (Q$_s$) from UGSS gauges in the Hudson estuary
976   watershed. The three estimates of sediment load are based on the (1) mean observed Q$_s$, (2) regression
977   between Q$_s$ and Q$_r$ during the Q$_s$ observations, and (3) the regression applied to the full Q$_r$ time series, if a
978   longer period is available. Similarly, discharge is averaged over the period of sediment load
979   measurements and over the full discharge record. Letters in first column correspond to locations shown
980   in Fig. 1 and data shown in Figs. 2 and 3. Totals of discharge and sediment load from the gauges flowing
981   into the tidal Hudson are shown, along with estimates farther seaward in the estuary scaled by watershed
982   area to account for ungauged watersheds. The watershed below Poughkeepsie and above The Battery is
983   assumed to have a specific sediment yield of 10 t km^{-2} yr^{-1}, based on values from nearby watersheds
984   (Yellen et al. 2014). Sediment yields are calculated based on the regression to the long-term discharge
985   records with tons in reference to metric tons here and throughout the paper.

Table 2	c	d	r^2
All stations	3.4	-.50	0.34
East of Hudson	2.7	-.38	0.92
West of Hudson	4.3	-.71	0.64

986

987 **Table 2.** Regression coefficients for sediment yield (Y, t km^{-2} y^{-1}) vs. watershed area (A, km^2), with the
988 form $Y = cA^d$. Fits are shown for all stations and separately for the stations to the east (Taconic Range)
989 and west (Catskill Mountains) of the Hudson.

Table 3	Stockport	Tivoli	Iona
Watershed area (km^2)	1340	1223	265
Number of dams	97	52	33
Trapped sediment mass (t)	3.7×10^5	6.4×10^5	1.8×10^4
Trapped mass per area (t km^{-2})	270	520	68
Typical watershed sediment yield (t km^{-2} yr^{-1})	60	100	10
Years of watershed supply trapped	4.5	5.2	6.8

990

991 **Table 3.** Impounded sediment mass estimates for the three study watersheds (Stockport, Tivoli, Iona).
992 Trapped sediment masses are calculated based impoundment categorization (trapping, run-of-river, or
993 non-source) and physical characteristics. For comparison, trapped masses are calculated as a percentage
994 of the expected watershed sediment yield over a period of 100 years.

Table 4				
Physical province	Trapped mass per area (t km^{-2})	Area (km^2)	Trapped mass (t)	Percentage of Lower Hudson watershed
Taconics (Stockport)	267	2610	7.0×10^5	18%
Catskills (Tivoli)	519	3120	1.6×10^6	22%
Hudson Highlands (Iona)	68	3170	2.2×10^5	22%
Hudson Lowlands	100	5360	5.4×10^5	38%
Total		14260	3.1×10^6	

995

996 **Table 4.** Impounded sediment mass estimates for the three study watersheds (Stockport, Tivoli, Iona).
997 Trapped sediment masses are calculated based impoundment categorization (trapping, run-of-river, or
998 non-source) and physical characteristics. For comparison, trapped masses are calculated as a percentage.

999

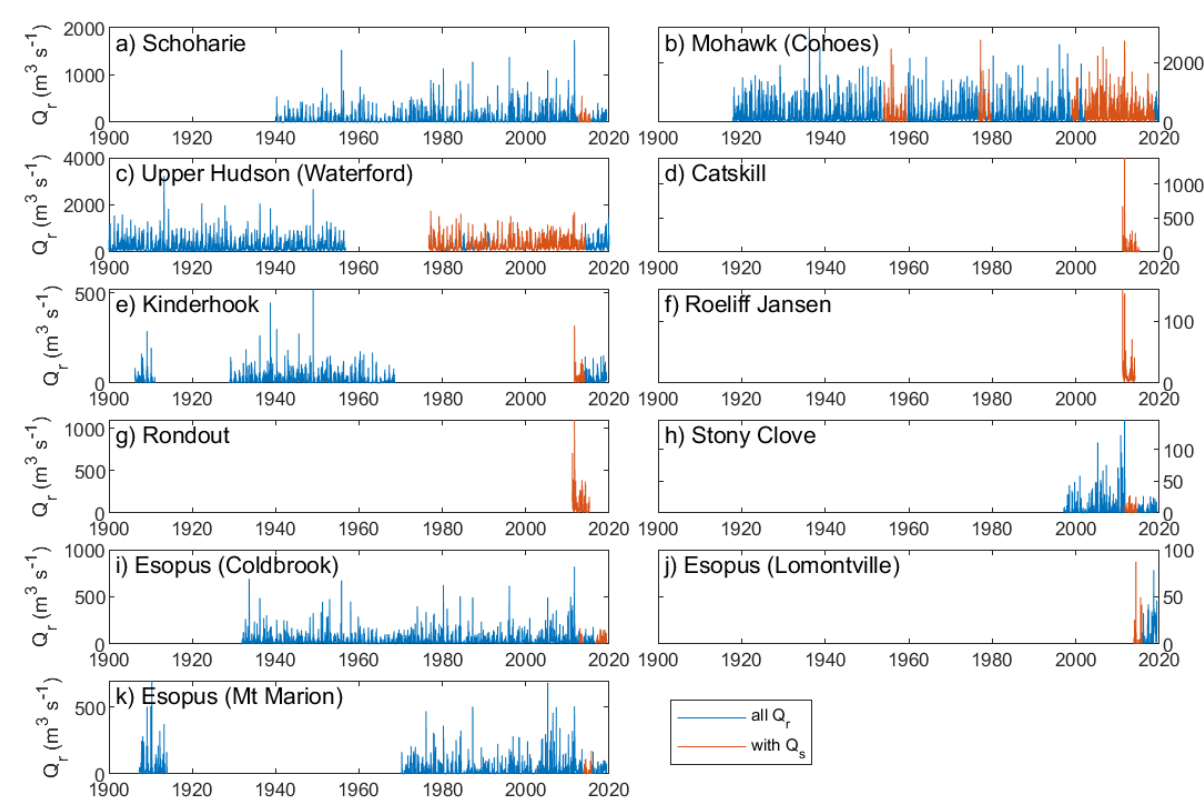| Table 5	Stockport	Tivoli	Iona
Shoal depth (H_s) (m)	6	10	12
Cross-sectional area (A) (m^2)	6×10^3	1×10^4	2×10^4
Mean velocity (U_0) (m s^{-1})	0.1	0.06	0.03
Advective length scale (L_{adv}) (km)			
Coarse silt (w_s = 2 mm/s)	9	9	5
Fine silt (w_s = 0.2 mm/s)	90	90	50
Clay (w_s = 0.02 mm/s)	900	900	500

1000

1001 **Table 5.** Scaling estimates for advective distances downstream from the source watersheds (Stockport,
1002 Tivoli, Iona) for different sediment size classes (coarse silt, fine silt, clay) for the representative model
1003 simulation period. Representative values for channel geometry and mean velocity listed here are used
1004 with Eqn. (4) and $C/C_0 = 0.05$.

1005

Figures

Figure 1. (A) Elevation in the lower Hudson River watershed (greyscale) with Upper Hudson River watershed in solid tan across the US states of New York (NY), Massachusetts (MA), Connecticut (CT), and New Jersey (NJ). Inset at bottom right shows location of the entire Hudson River watershed with respect to NY. USGS gauges (red dots) are labeled with letters corresponding to Table 1 and Fig. 2. Watersheds in which dams were studied in detail are outlined in orange (Stockport), yellow (Esopus; Stoney Creek; Saw Kill), and green (Doodletown-Popolopen; Canopus Creek). (B) Stockport Creek watershed with all NID dams classified by category: active sediment traps; non-sources of sediment (breached, spring-fed ponds, natural lakes), and run-of-river sites. See methods for classification criteria. (C) Physiographic provinces of New York State and New Jersey with the Lower Hudson River watershed's (hashed area) main provinces labeled (see text and Table 4 for details). The broader Hudson River basin is shaded grey.

1019

Figure 2

1020

1021 **Figure 2.** Volumetric discharge at USGS gauging stations in the Hudson River estuary watershed.
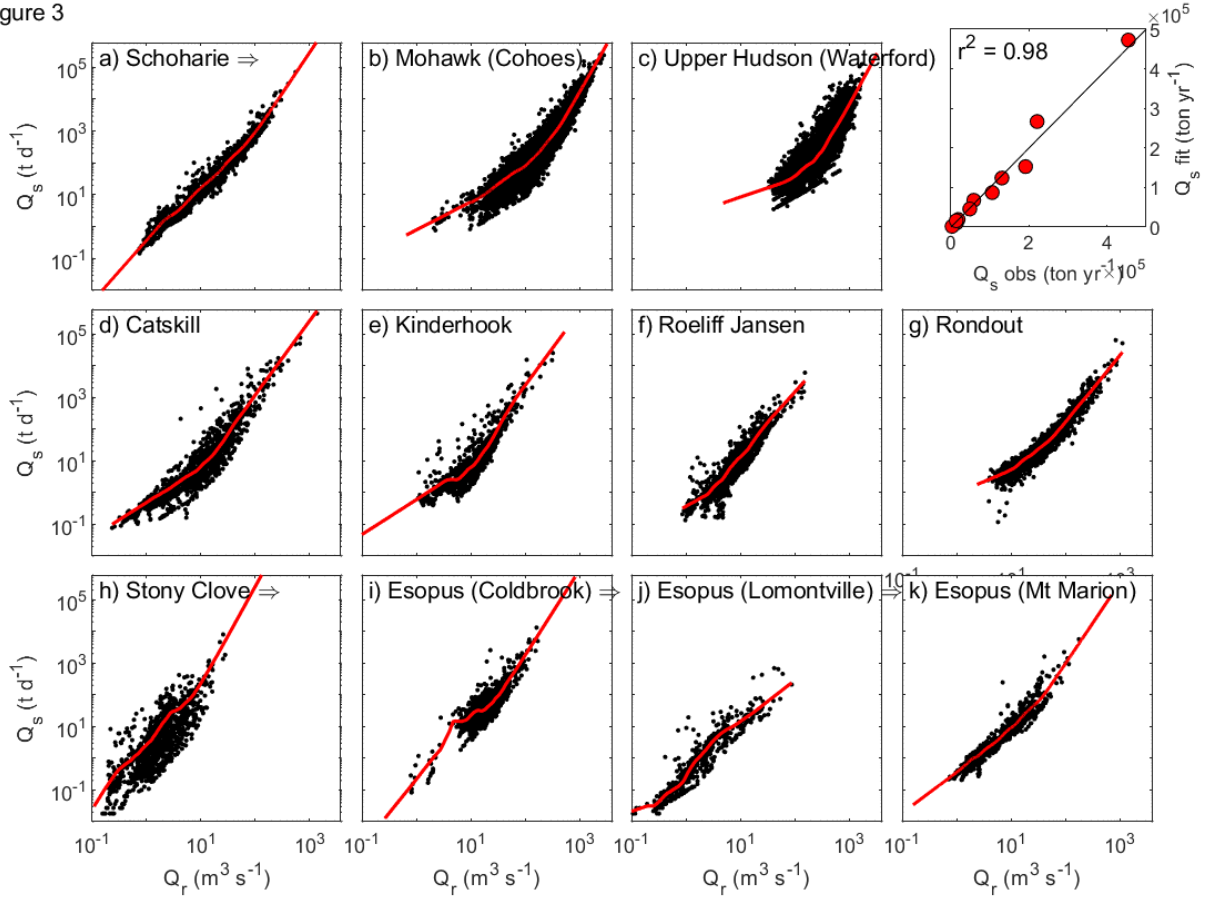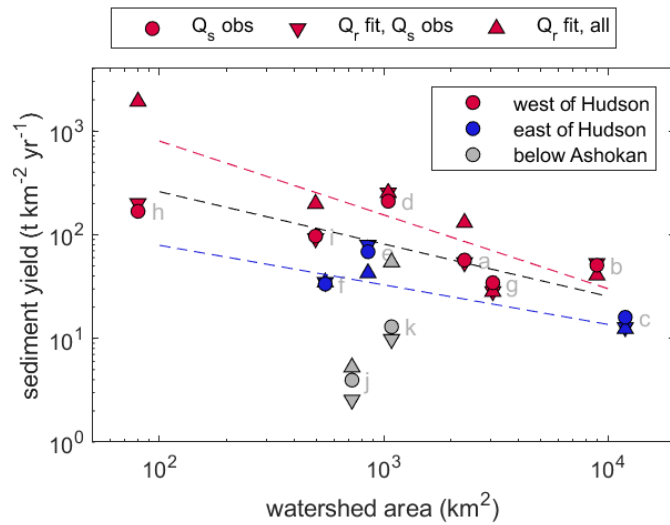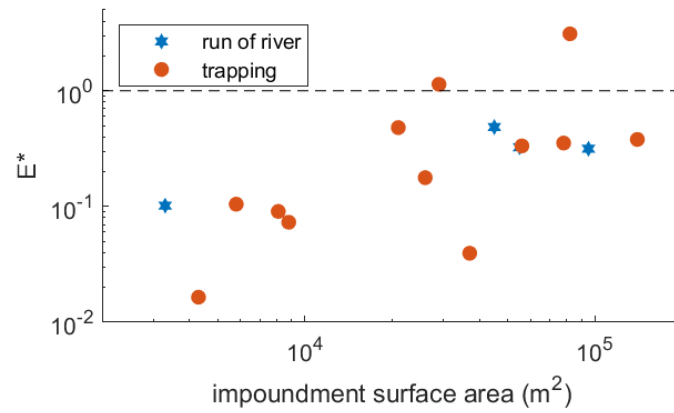1022 Periods highlighted in red also have sediment discharge measurements.

Figure 3

Figure 3. Sediment discharge vs. volumetric discharge at USGS gauging stations. Red lines are LOWESS fits, and the total calculated sediment load vs. observed for all the stations is shown in the upper right panel. Stations located in the same subwatershed are in panels adjacent to stations farther downstream and labeled with "→".

28

Figure 4

1028

1029   **Figure 4.** Sediment yield vs. watershed area. Sediment yields are calculated based on observed sediment
1030   discharge, the LOWESS regression fit to Q_r during the sediment discharge observations, and from the
1031   regression over the full record of Q_r. Stations are labeled as being west or east of the Hudson, and the two
1032   stations on the Esopus below the Ashokan Reservoir are noted separately. The letters adjacent to each set
1033   of points correspond to the subpanels in Figure 3. Regression lines (Eqn. 1) are shown for all stations
1034   (black) and just those east (blue) or west (red) of Hudson; regression coefficients are listed in Table 2.

Figure 5

Figure 5. E*, or the ratio of the mass of sediment in an impoundment potentially released by dam removal to the annual sediment load from the watershed (Eqn. 2) vs. impoundment surface area for the study sites. Run-of-river impoundments are distinguished from trapping impoundments, and tend to have lower E* values.
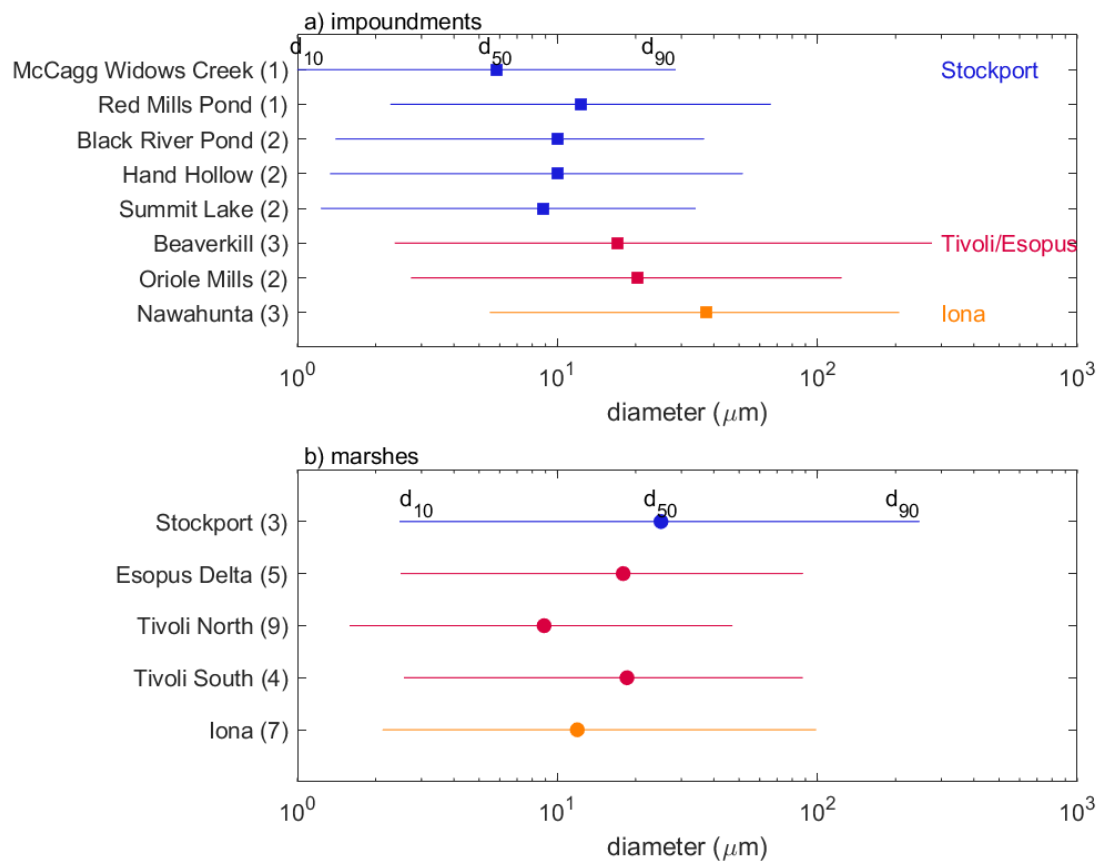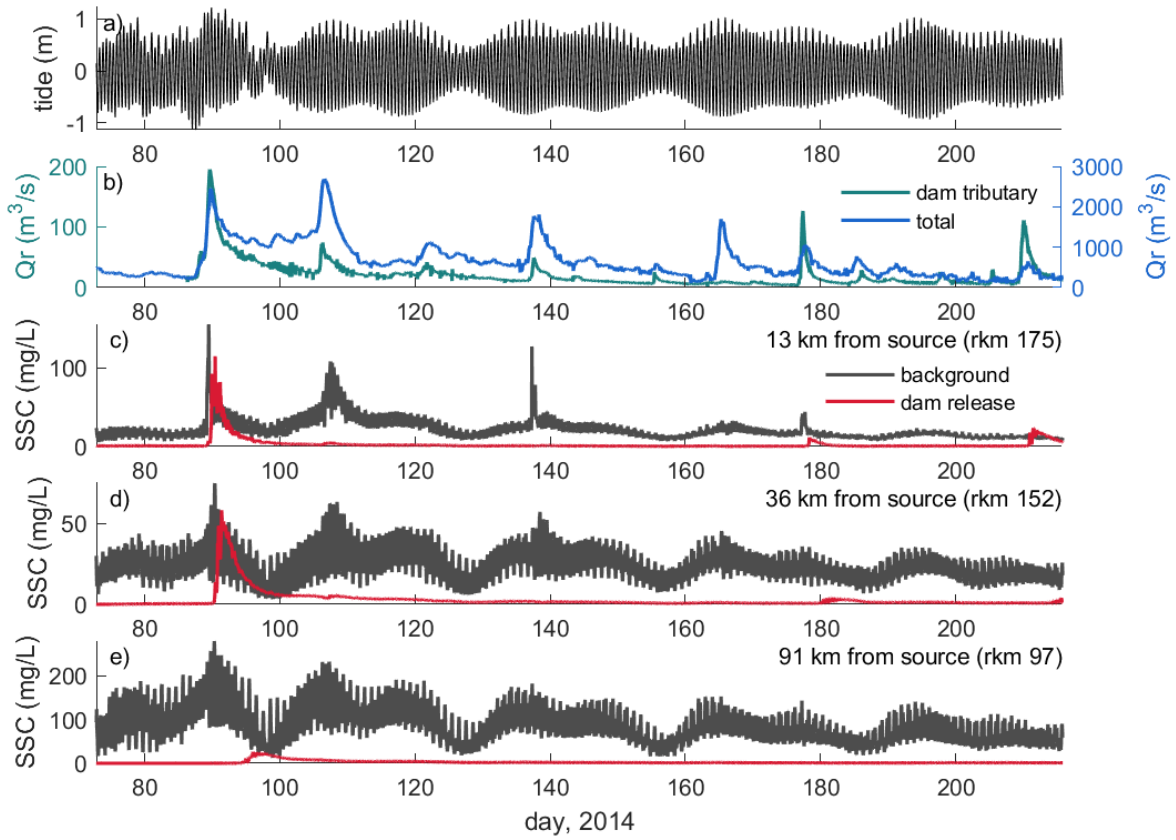
Figure 6

Figure 6. Particle size distributions from a) impoundments and b) marshes. Marker shows the average d_{50}, and the line shows d_{10} to d_{90}. Impoundment locations are grouped by subwatershed, and the number of cores from each is noted in parentheses.
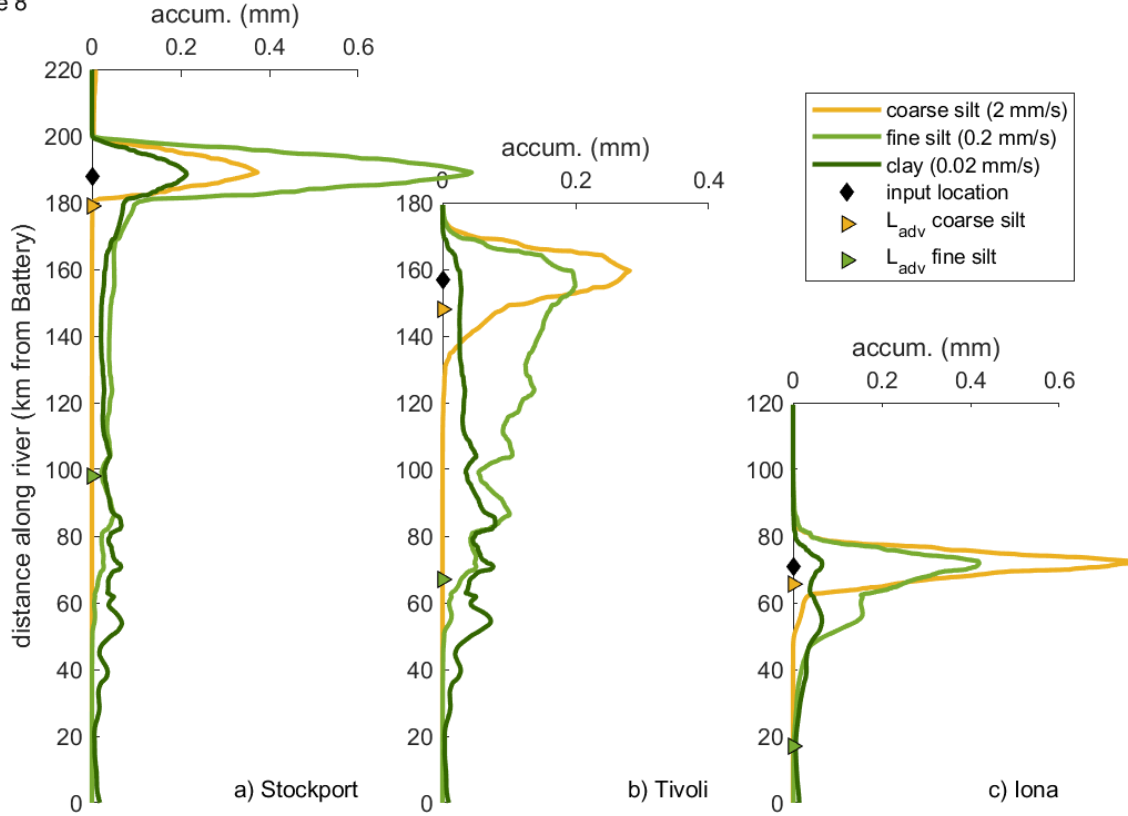
Figure 7

Figure 7. Suspended sediment concentrations in estuary from sediment release in model with forcing from spring 2014. a) Water level during the simulation; b) total discharge (blue) and discharge from Kinderhook Creek (teal), the tributary with the simulated dam removal; c) near-surface SSC at 13 km seaward from the tributary input, separating the dam removal inputs (red) from all other sources including other tributaries and bed resuspension; d) SSC 36 km seaward from the dam removal input; e) SSC 91 km from the input.

Figure 8. Along-estuary deposition from sediment releases. a) Coarse silt, fine silt, and clay-sized particle deposition vs distance along the estuary for the simulated dam sediment release near Stockport marsh. Black diamond marks input location, and triangles mark the advective length scales for each sediment size class calculated from Eqn. 4. b) sediment deposition by size class for inputs from near Tivoli marsh, and c) near Iona Island marsh.